Reaction of H_2 with $IrHCl_2P_2$ (P = P^iPr_3 or P^tBu_2Ph): Stereoelectronic Control of the Stability of Molecular H_2 Transition Metal Complexes

Alberto Albinati,[⊖] Vladimir I. Bakhmutov,[‡] Kenneth G. Caulton,[⊥] Eric Clot,[∥] Juergen Eckert,[○] Odile Eisenstein,[∥] Dmitry G. Gusev,[‡] Vladimir V. Grushin,[●] Bryan E. Hauger,[⊥] Wim T. Klooster,[§] Thomas F. Koetzle,[§] Richard K. McMullan,[§] Terence J. O'Loughlin,[§] Michel Pélissier,[▽] John S. Ricci,[§] Michael P. Sigalas,[∥,†] and Alexey B. Vymenits[‡]

Contribution from the Department of Chemistry, Indiana University, Bloomington, Indiana 47405, NMR Laboratory of the Institute of Organo-Element Compounds, Russian Academy of Sciences, Moscow, Russia, Department of Chemistry, Brookhaven National Laboratory, Upton, Long Island, New York 11973, Laboratoire de Chimie Théorique, Université de Paris-Sud, 91405 Orsay, France, Department of Chemistry, University of Ottawa, Ottawa, Ontario K1N 6N5, Canada, Los Alamos National Laboratory, Los Alamos, New Mexico 87545, Istituto di Chimica Farmaceutica, Universita di Milano, I-20131 Milano, Italy, and Laboratoire de Catalyse en Chimie Organique, Université de Poitiers, 86022 Poitiers, France

Received March 10, 1993

Abstract: $IrHCl_2P_2$ (P = P^iPr_3) reacts rapidly with H_2 at 25 °C to set up an equilibrium where H_2 binds *trans* to the original hydride ligand (*trans*-**2**). A second slower reaction forms $IrH(H_2)Cl_2P_2$ (*cis*-**2**), where the *cis* disposition of the chlorides, and also H *cis* to H_2, was established by neutron diffraction. This molecule (unlike *trans*-**2**), shows rapid site exchange between coordinated H and H_2. *cis*-**2** can be induced to lose HCl to form $Ir(H)_2ClP_2$ (**3**). The structure of $Ir(H)_2Cl(P^iBu_2Ph)_2$, an analog of **3**, was shown by neutron diffraction to have a planar H_2IrCl in a Y shape, with Cl at the base of the Y and a H–Ir–H angle of only 73°. ECP *ab initio* calculations of $IrH_2Cl(PH_3)_2$ show that the Y shape with a H–Ir–H angle close to the experimental value has the minimum energy. They also show that the *trans*-**2** isomer of $IrH(H_2)Cl_2(PH_3)_2$ is less stable than the *cis*-**2** isomer by 10.3 kcal/mol. The Ir–H_2 interaction is stronger in *cis*-**2**. The rotational barrier has been calculated in the two isomers as 2.3 (*trans*) and 6.5 (*cis*) kcal/mol. In agreement with the experimental structure, the H–H bond is found to eclipse preferentially the Ir–H bond in *cis*-**2**. The calculations also show that the Ir–H_2 bond dissociation energy is greater in *cis*-**2**. It thus appears that the binding ability of a metal fragment not only depends on its ligands but is also linked in a subtle way to its stereochemistry. The J(HD) value for coordinated H_2 in *cis*-**2** is 12 ± 3 Hz. The implication of this small value and of a T_{1min}(200 MHz) of 38 ms is an H/H distance of 1.07–1.35 Å, which compares to the neutron diffraction distance of 1.11(3) Å. The Ir–H distances of *cis*-**2** are unprecedented in that the hydride–Ir distance (1.584(13) Å) is not shorter than the distances to the H_2 hydrogens (1.537(19) and 1.550(17) Å). One of the H_2 hydrogens interacts with chloride of an adjacent molecule to give an infinite hydrogen-bonded polymer. An inelastic neutron scattering spectroscopic study on solid $IrHCl_2(H_2)(P^iPr_3)_2$ sets a *lower limit* on the rotational barrier of the $Ir(H_2)$ unit of 2.0 kcal/mol. *Ab initio* calculations on $IrHCl_2(H_2)(PH_3)_2$ yield a H–H distance in these two isomers of 0.81 and 1.4 Å, respectively, showing that the moiety $IrHCl_2(PH_3)_2$ with chlorides mutually *cis* is a much stronger reducing agent than that with chlorides *trans* (and thus H *trans* to H_2). Crystallographic data: For *cis*-**2** (at 15K), a = 13.008(4) Å, b = 11.296 (4) Å, c = 16.095(4) Å in space group $Pna2_1$ (Z = 4). For $Ir(H)_2Cl(P^iBu_2Ph)_2$ (at 15K), a = 8.236(2) Å, b = 17.024(6) Å, c = 20.528(10) Å, β = 96.27(4)° in space group $P2_1/c$ (Z = 4).

Introduction

The heterolytic splitting of H_2, as exemplified by eq 1 (M =

$$MCl_3(PR_3)_n + H_2 \xrightarrow{PR_3} MHCl_2(PR_3)_3 + HCl \qquad (1)$$

Rh or Ir), is a reaction which has considerable significance for forming a metal hydride from an economical hydrogen source and under mild conditions. The subject has been reviewed,[1] but mechanistic insights remain few in number. Groups other than halide can be eliminated with H^+, and added Brønsted base is sometimes beneficial to the rate and/or thermodynamics of this H_2 heterolysis. The reaction is found mainly for the later transition elements, and among those, the d^6 electron configuration (eq 1) is frequently involved. We suggest that the fact that molecular H_2 is most often found in d^6 metal complexes[2] may be very relevant to understanding this heterolytic splitting of H_2. This proposal is strengthened by the fact that coordinated H_2 has been shown in numerous cases to be Brønsted-acidic[3] (eq 2), a reaction which

[⊖] Universita de Milano.
[‡] Russian Academy of Sciences.
[⊥] Indiana University.
[∥] Université de Paris-Sud.
[○] Los Alamos National Laboratory.
[●] University of Ottawa.
[§] Brookhaven National Laboratory.
[▽] Université de Poitiers.
[†] Permanent Address: Laboratory for Applied Quantum Chemistry, University of Thessaloniki, Thessaloniki, Greece.

(1) Brothers, P. J. *Prog. Inorg. Chem.* **1981**, *28*, 1.
(2) Jessop, P. G.; Morris, R. J. *Coord. Chem. Rev.* **1992**, *121*, 155.

0002-7863/93/1515-7300$04.00/0

Table I. Temperature Dependence of the Ratio[a] R = [1]/[*cis*-2] in Toluene under 1 atm of Ar or H_2

under Ar			under H_2		
T, °C	thermostating time, h	R	T, °C	thermostating time, h	R
40	17.5	0.32			
56	3	0.64	56	6	0.18
56	8.5	0.64	80	4	0.24
75	3	1.13	98	4	0.43
83	6	2.12			

[a] Calculated from the integral intensities of the phosphine proton resonances at 2.47 (*cis*-**2**) and 3.03 (**1**) (error <10%).

itself is a heterolysis of H_2. We report here results which further support this conjecture.

$$M(H_2) + B \rightarrow MH^- + BH^+ \quad (2)$$

Experimental Section

All preparations and handling of complexes were carried out under an atmosphere of H_2 or argon (oxygen free). $IrHCl_2(P^iPr_3)_2$, **1**,[4] and D_2[6] were synthesized by literature methods.

Unless otherwise stated, all NMR data reported in this paper were obtained on a Bruker WP-200 SY spectrometer. ^1H and ^2H chemical shifts were measured with the solvent resonance as reference. Relaxation time (T_1) experiments employed the inversion recovery method (180°–τ–90° pulse sequence). All temperatures were calibrated by using ^1H NMR chemical shifts of methanol.

***cis*-$IrHCl_2(H_2)(P^iPr_3)_2$(*cis*-2).**[7] A mixture of $Ir(H)Cl_2(P^iPr_3)_2$ (1.80 g) and benzene (20 mL, freshly distilled from sodium benzophenone ketyl) was stirred under dry H_2 (1 atm) in a 150-mL Schlenk tube equipped with a mercury bubbler at 50–55 °C (oil bath) for 8 h. After the solution stood at room temperature (22 °C) overnight, a mixture of the dihydrogen complex (large yellowish crystals) and the starting deep-purple monohydride precipitated. The mixture was kept at 35 °C until the purple crystals dissolved (3.5 h) and left at room temperature for 18 h. Since small amounts of the starting monohydride precipitated again, the mixture was kept under H_2 at 35 °C for 5 h, after which no purple crystals precipitated from the orange-yellow solution upon cooling. Pentane (H_2-saturated; 20 mL) was added, and the mixture was kept in an ice bath for 1 h. The golden yellow crystals were separated, washed with H_2-saturated pentane (4 × 10 mL), and thoroughly dried by a flow of pure, dry H_2. The yield of *cis*-**2** was 1.45 g (81.4%). The complex can be stored under argon in a sealed glass tube for at least 1.5 years. Solution equilibration of this compound with **1** is described by the data in Table I. IR (Nujol, cm^{-1}): 2264 (s), 2197 (m).

Crystallization of $IrH_2Cl(P^tBu_2Ph)_2$. Solid $IrH_2Cl(P^tBu_2Ph)_2$[8] (0.4 g) was dissolved in 4 mL of THF to yield a homogeneous orange-brown solution. The THF solution was layered with 5 mL of hexanes. After 1 week, large orange crystals were isolated by decanting the mother liquor and drying under vacuum.

Neutron Diffraction Study of $IrH_2ClP(Ph)(^tBu)_2$ at 15 K. The crystal selected for neutron diffraction study exhibited forms {100, 010, 011} and had the dimensions 2.5 × 1.7 × 0.8 mm and 2.7 mm^3, where the longest dimension is coincident with the a axis. The sample was covered in a protective film of halocarbon grease, mounted on its c axis to an aluminum pin, and sealed inside an aluminum cannister under helium gas during measurements. The data were collected on the four-circle diffractometer at port H6S of the Brookhaven high flux beam reactor. The neutron beam, monochromated by Ge(220) planes in transmission geometry, was of wavelength of 1.1584(1) Å as calibrated against a KBr crystal (a_0 = 6.6000 Å at 295 K). During the 3 weeks of measurements, the crystal temperature was held at 15 ± 0.1 K inside a two-stage DISPLEX helium cryostat. The lattice parameters were determined by a least-squares fit of $\sin^2\theta$ values for 32 reflections within the range $40° < 2\theta < 54°$, to yield a = 8.236(2) Å, b = 17.024(6) Å, c = 20.528(10) Å, β = 96.27(4)°, and space group $P2_1/c$ (Z = 4). Intensity data in one quadrant [$\pm h,\bar{k},\bar{l}$; $|h| \le 9, |k| \le 20, |l| \le 24$; $0.05 < \sin\theta/\lambda < 0.70$ Å^{-1}] were measured with scan widths of $\Delta 2\theta = 3.0°$ for $\sin(\theta/\lambda) \le 0.43$ Å^{-1} and $\Delta 2\theta = (1.291 + 2.533 \tan\theta)°$ for $\sin(\theta/\lambda) > 0.43$ Å^{-1}. The intensities of two reflections [1, $\bar{8}$, 12; 6, $\bar{5}$, $\bar{3}$] monitored at regular intervals showed no systematic variations. Integrated intensities I_0 and variances $\sigma^2(I_0)$ were derived from the scan profiles as described previously.[9] Absorption corrections[10,11] were applied using μ_n = 3.352 cm^{-1} evaluated from μ/ρ = 2.641 $cm^2\ g^{-1}$ for hydrogen[12] and literature[13] μ/ρ values for non-hydrogen atoms. Minimum and maximum transmission factors were 0.488 and 0.776, respectively. Averaging F_o^2 values of 166 symmetry-related pairs of reflections resulted in an internal agreement index of 0.039 and yielded 5154 independent observations, of which 707 were negative, 27 being less than $-2\sigma(F_o^2)$.

For the refinement model, starting nuclear parameters of non-hydrogen atoms were taken from a room-temperature X-ray analysis. Coherent neutron-scattering lengths (*fm*) for H (−3.7409), C (6.6484), P (5.13), Cl (9.579), and Ir (10.6) were taken from a tabulation.[14] The hydrogen atoms were located in successive difference maps interspersed with parameter refinements by differential Fourier methods. Refinement of the completed model of 80 independent atoms was carried out by full-matrix least-squares methods with the program UPALS.[15] The quantity $\sum w|F_o^2 - F_c^2|^2$ was minimized with weights $w = [\sigma^2(F_o^2) + (0.02F_o^2)^2]^{-1}$, summing over the 5154 independent observations. The variable parameters were coordinates, isotropic B for all atoms, one scale factor, and the isotropic secondary extinction parameter for a type I crystal.[16] The extinction parameter was omitted from the list after it failed to assume a significantly non-zero value in refinement, which left 321 parameters. The refinement converged ($\Delta p_i/\sigma(p_i) < 0.01$) with fit indices $R(F_o^2)$ = 0.211, $wR(F_o^2)$ = 0.194, and S = 1.67 based on all reflections and $wR(F_o)$ = 0.114 based on 4447 reflections with $F_o^2 > 0.^{17}$ In the final ΔF map, the largest $|\Delta\rho|$ errors were <5% of the peak maximum for carbon in the ρ_0 map. Results of the structure determination are shown in Tables II and III, Figures 3 and 4, and the supplementary material.

Neutron Diffraction Study of $IrHCl_2(H_2)(P^iPr_3)_2$ at 15 K. General methods and absorption and scattering parameters were identical with those used above. The crystal selected for neutron diffraction study exhibited forms {0.11, 100} and had the dimensions 5.8 × 1.1 × 1.1 mm and 7.5 mm^3, where the longest dimension was coincident with the a axis. The sample was covered in a protective film of halocarbon grease, mounted on its (100) face to an aluminum pin, and sealed inside an aluminum cannister under helium gas during measurements (15 K). The lattice parameters were determined by a least-squares fit of $\sin^2\theta$ values for 32 reflections within the range $42° < 2\theta < 51°$ to yield a = 13.008(4) Å, b = 11.296(4) Å, c = 16.095(4) Å in space group $Pna2_1$ (Z = 4). Intensity data in two octants [$h,\bar{k},l$; $h \le 18, |k| \le 16, l \le 22$; $\sin(\theta/\lambda) < 0.71$ Å^{-1}] and [h,k,l; $h \le 13, k \le 14, l \le 19$; $\sin(\theta/\lambda) < 0.62$ Å^{-1}] were measured with scan widths of $\Delta 2\theta = 3.0°$ for $\sin(\theta/\lambda) \le 0.36$ Å^{-1} and $\Delta 2\theta = (1.768 + 2.576 \tan\theta)°$ for $\sin(\theta/\lambda) > 0.36$ Å^{-1}. The intensities of four reflections [4,$\bar{7}$,3; 3,2,11; 0,$\bar{8}$,8; 0,0,14] monitored at regular intervals showed no systematic variations. Minimum and maximum transmission factors were 0.354 and 0.713, respectively. Averaging F_o^2 values of 2134 symmetry-related pairs of reflections resulted in an internal agreement index of 0.055 and yielded 3638 independent observations, of which 463 were negative, 5 being less than $-2\sigma(F_o^2)$. Seventeen reflections were omitted from the refinement because they very likely were affected by the aluminum powder lines caused by the pin and cannister.

(3) Chinn, M. S.; Heinekey, D. M. *J. Am. Chem. Soc.* **1990**, *112*, 5166. Cappellani, E. P.; Maltby, P. A.; Morris, R. H.; Schweitzer, A. T.; Steele, M. R. *Inorg. Chem.* **1989**, *28*, 4437. Johnson, T. J.; Caulton, K. G. *J. Am. Chem. Soc.* **1992**, *114*, 2725.

(4) Grushin, V. V.; Vymenits, A. B.; Volpin, M. E. *J. Organomet. Chem.* **1990**, *382*, 185.

(5) Wender, I.; Friedel, R. A.; Orchin, M. *J. Am. Chem. Soc.* **1949**, *71*, 1140.

(6) Brauer, G. In *Handbook of Preparative Inorganic Chemistry, 2nd ed.*; Academic Press: New York 1963; Vol. 1.

(7) Gusev, D. G.; Bakhmutov, V. I.; Grushin, V. V.; Volpin, M. E. *Inorg. Chim. Acta* **1990**, *177*, 115.

(8) Empsall, H. D.; Hyde, E. M.; Mentzer, E.; Shaw, B. L.; Uttley, M. F. *J. Chem. Soc., Dalton Trans.* **1976**, 2069.

(9) McMullan, R. K.; Epstein, J.; Ruble, J. R.; Craven, B. M. *Acta Crystallogr.* **1979**, *B35*, 688.

(10) de Meulenaer, J.; Tompa, H. *Acta Crystallogr.* **1965**, *19*, 1014.

(11) Templeton, L. K.; Templeton, D. H. *Abstr. Am. Crystallogr. Assoc. Meet.*, Storrs, CT, 1973; p 143.

(12) Koetzle, T. F.; McMullan, R. K., unpublished results.

(13) *International Tables for X-ray Crystallography*; MacGillavry, C. H., Rieck, G. D., Eds.; Kynoch: Birmingham, 1968; Vol. III, pp 197–198.

(14) Koester, L. In *Springer Tracts in Modern Physics*; Höhler, G., Ed.; Springer: Berlin, 1977; Vol. 80, Neutron Physics, p 36.

(15) Lundgren, J.-O. *UPALS*; A Full-matrix Least-squares Refinement Program; Report UUICB13-4-05, Institute of Chemistry, University of Uppsala, Uppsala, Sweden, 1982.

(16) Becker, P. J.; Coppens, P. *Acta Crystallogr.* **1974**, *A30*, 129.

(17) $R(F_o^2) = \sum\Delta/\sum|F_o^2|$; $wR(F_o^2) = [\sum w\Delta^2/\sum wF_o^4]^{1/2}$; $S = [\sum w\Delta^2/(n-p)]^{1/2}$, where $\Delta = |F_o^2 - F_c^2|$, and n and p are the numbers of observations and parameters, respectively; $wR(F_o) = [\sum w'|F_o - |F_c||^2/\sum w'F_o^2]^{1/2}$, $w' = w/2F_o$.

Table II. Bond Lengths (Å) in $Ir(H)_2Cl(P^tBu_2Ph)_2$

Ir–Cl	2.410(4)	C212–C213	1.404(7)
Ir–P1	2.325(7)	C213–C214	1.404(7)
Ir–P2	2.326(7)	C214–C215	1.385(8)
Ir–HIr1	1.512(14)	C215–C216	1.396(7)
Ir–HIr2	1.553(14)	C221–C222	1.552(7)
P1–C111	1.832(8)	C221–C223	1.532(8)
P1–C121	1.899(8)	C221–C224	1.541(7)
P1–C131	1.909(8)	C231–C232	1.545(7)
P2–C211	1.849(8)	C231–C233	1.543(7)
P2–C221	1.895(8)	C231–C234	1.531(7)
P2–C231	1.894(8)	C112–H112	1.057(13)
C111–C112	1.411(7)	C113–H113	1.076(13)
C111–C116	1.392(7)	C114–H114	1.062(13)
C112–C113	1.403(8)	C115–H115	1.067(14)
C113–C114	1.403(8)	C116–H116	1.085(13)
C114–C115	1.396(7)	C122–H122a	1.090(13)
C115–C116	1.414(8)	C122–H122b	1.082(15)
C121–C122	1.543(7)	C122–H122c	1.079(13)
C121–C123	1.548(7)	C123–H123a	1.099(14)
C121–C124	1.542(7)	C123–H123b	1.102(12)
C131–C132	1.543(7)	C123–H123e	1.056(14)
C131–C133	1.534(8)	C124–H124a	1.082(16)
C131–C134	1.559(7)	C124–H124b	1.101(14)
C211–C212	1.413(7)	C124–H124c	1.093(13)
C211–C216	1.411(7)	C132–H132a	1.061(15)
C132–H132b	1.093(13)	C223–H223a	1.111(13)
C132–H132c	1.061(13)	C223–H223b	1.064(14)
C133–H133a	1.114(13)	C223–H223c	1.116(14)
C133–H133b	1.070(14)	C224–H224a	1.104(14)
C133–H133c	1.095(14)	C224–H224b	1.097(14)
C134–H134a	1.111(14)	C224–H224c	1.074(13)
C134–H134b	1.053(16)	C232–H232a	1.100(14)
C134–H134c	1.082(13)	C232–H232b	1.044(13)
C212–H212	1.097(13)	C232–H232c	1.068(15)
C213–H213	1.017(15)	C233–H233a	1.050(15)
C214–H214	1.091(13)	C233–H233b	1.107(14)
C215–H215	1.092(13)	C233–H233c	1.098(14)
C216–H216	1.033(14)	C234–H234a	1.078(14)
C222–H222a	1.115(13)	C234–H234b	1.088(14)
C222–H222b	1.063(15)	C234–H234c	1.073(13)
C222–H222c	1.071(14)	HIr1–HIr2	1.82(2)

Table III. Bond Angles (deg) in $Ir(H)_2Cl(P^tBu_2Ph)_2$

Cl–Ir–P1	93.1(2)	C111–C112–C113	120.6(4)
Cl–Ir–P2	94.5(2)	C112–C113–C114	119.8(4)
P1–Ir–P2	172.3(2)	C113–C114–C115	120.1(5)
Cl–Ir–HIr1	131.1(5)	C114–C115–C116	119.7(4)
P1–Ir–HIr1	86.1(5)	C111–C116–C115	120.8(4)
P2–Ir–HIr1	87.9(6)	P1–C121–C122	107.2(3)
Cl–Ir–HIr2	156.2(5)	P1–C121–C123	113.6(4)
P1–Ir–HIr2	85.8(5)	P1–C121–C124	111.3(4)
P2–Ir–HIr2	87.7(5)	C122–C121–C123	107.3(4)
HIr1–Ir–HIr2	72.7(7)	C122–C121–C124	107.9(4)
Ir–P1–C111	111.8(3)	C123–C121–C124	109.4(4)
Ir–P1–C121	114.9(3)	C132–C131–C133	107.9(4)
Ir–P1–C131	110.8(3)	C132–C131–C134	107.8(4)
C111–P1–C121	101.4(4)	C133–C131–C134	108.0(4)
C111–P1–C131	108.2(3)	P2–C211–C212	117.1(4)
C121–P1–C131	109.1(3)	P2–C211–C216	124.7(4)
Ir–P2–C211	112.7(3)	C212–C211–C216	118.1(4)
Ir–P2–C221	110.4(3)	C211–C212–C213	121.3(4)
Ir–P2–C231	114.5(3)	C212–C213–C214	119.2(5)
C211–P2–C221	105.9(3)	C213–C214–C215	119.9(4)
C211–P2–C231	102.0(3)	C214–C215–C216	121.3(5)
C221–P2–C231	110.6(4)	C211–C216–C215	120.2(5)
P1–C111–C112	115.9(4)	P2–C221–C222	108.8(4)
P1–C111–C116	125.0(4)	P2–C221–C223	117.7(4)
C112–C111–C116	119.0(4)	P2–C221–C224	107.6(4)
C222–C221–C223	107.9(4)	P2–C231–C234	109.9(3)
C222–C221–C224	106.8(4)	C232–C231–C233	106.6(4)
C223–C221–C224	107.6(4)	C232–C231–C234	109.2(4)
P2–C231–C232	106.5(4)	C233–C231–C234	109.6(4)
P2–C231–C233	114.7(4)		

For the refinement model, starting nuclear parameters of non-hydrogen atoms were taken from the 153K X-ray analysis.[18] The hydrogen atoms were located in successive difference maps interspersed with parameter refinements by differential Fourier methods. Refinement of the completed model of 68 independent atoms minimized the quantity $\sum w|F_o^2 - F_c^2|^2$, using weights $w = [\sigma^2(F_o^2) + (0.02F_o^2)^2]^{-1}$, summing over the 3621 independent observations. The variable parameters were coordinates, isotropic B for all atoms, one scale factor, and the isotropic secondary extinction parameter for a type I crystal. The z coordinate of iridium was fixed to define the origin. The extinction parameter was omitted from the list after it failed to assume a significantly non-zero value in refinement, which left 272 parameters. The refinement converged ($\Delta p_i/\sigma(p_i) < 0.01$) with fit indices of $R(F_o^2) = 0.296$, $wR(F_o^2) = 0.196$, and $S = 1.31$ based on all reflections and $wR(F_o) = 0.119$ based on 3158 reflections with $F_o^2 > 0$.[19] In the final ΔF map, the largest $|\Delta\rho|$ errors were <4% of the peak maximum for carbon in the ρ_0 map. Results are shown in Tables IV and V, Figure 10, and the supplementary material.

Table IV. Bond Lengths (Å) in $IrHCl_2(H_2)(P^iPr_3)_2$

HIr2–HIr1	1.11(3)	C5–H51	1.095(26)
Ir–Cl1	2.496(6)	C5–H52	1.022(24)
Ir–Cl2	2.445(6)	C5–H53	1.078(24)
Ir–P1	2.359(8)	C6–H61	1.252(25)
Ir–P2	2.364(8)	C6–H62	1.083(23)
Ir–HIr1	1.550(17)	C6–H63	1.036(22)
Ir–HIr2	1.537(19)	C7–H71	1.109(18)
Ir–HIr3	1.584(13)	C8–H81	1.201(34)
P1–C1	1.830(11)	C8–H82	1.045(22)
P1–C4	1.867(10)	C8–H83	1.074(20)
P1–C7	1.846(9)	C9–H91	1.050(18)
P2–C10	1.802(13)	C9–H92	1.069(24)
P2–C13	1.885(12)	C9–H93	1.095(21)
P2–C16	1.847(10)	C10–H101	1.192(36)
C1–C2	1.572(11)	C11–H111	1.174(33)
C1–C3	1.515(10)	C11–H112	1.222(37)
C4–C5	1.539(10)	C11–H113	0.823(38)
C4–C6	1.510(10)	C12–H121	1.115(25)
C7–C8	1.531(11)	C12–H122	0.982(34)
C7–C9	1.521(11)	C12–H123	1.070(31)
C10–C11	1.534(18)	C13–H131	1.160(23)
C10–C12	1.528(13)	C14–H141	0.943(38)
C13–C14	1.523(14)	C14–H142	1.060(32)
C13–C15	1.479(14)	C14–H143	1.048(30)
C16–C17	1.499(11)	C15–H151	1.050(29)
C16–C18	1.557(12)	C15–H152	1.055(33)
C1–H11	1.094(18)	C15–H153	1.083(39)
C2–H21	1.151(22)	C16–H161	1.105(17)
C2–H22	1.045(23)	C17–H171	1.107(20)
C2–H23	1.077(25)	C17–H172	1.152(24)
C3–H31	1.074(22)	C17–H173	1.096(22)
C3–H32	1.117(25)	C18–H181	0.988(26)
C3–H33	1.128(22)	C18–H182	1.080(28)
C4–H41	1.101(16)	C18–H183	1.074(30)

Computational Methods. Computations on $IrH_2Cl(PH_3)_2$ followed the method reported.[20] For $IrHCl_2(PH_3)_2$ and $IrH(H_2)Cl_2(PH_3)_2$ an effective core potential (ECP) was used for Ir, Cl, and P. For Ir, the ECP of Hay and Wadt which includes the 5s and 5p electrons in the valence shell was chosen[21] with a (6s6p4d) Gaussian a basis set contracted into [3111/3111/211].[20] For Cl and P we have used the ECP of Barthelat *et al.*[22] and of Stevens and Basch[23] respectively with the associated (4s,4p) basis set contracted into the [2s,2p] double-ζ basis set. For the hydrogen atoms of PH_3, a (4s) basis set contracted into [1s] was chosen.[24] For the H atom bonded to the metal in $IrHCl_2(PH_3)_2$ a (4s) Gaussian basis set contracted into the [31] basis set of Huzinaga[25] was used. For the H atoms bonded to the metal in $IrH(H_2)Cl_2(PH_3)_2$, a (5s) Gaussian basis set contracted into the [311] basis set of Huzinaga[25] and augmented by a p polarization function ($\zeta = 1.0$) was used. The HF/MP2 calculations were done with the GAMESS program.[26]

(18) Yanovsky, A.; Struchkov, Y. T., private communication.
(19) Another refinement was performed varying anisotropic displacement parameters for all atoms, 612 parameters. This resulted in $R(F_o^2) = 0.248$; $wR(F_o^2) = 0.156$; $wR(F_o) = 0.096$; $S = 1.10$. Several atoms were non-positive definite, although not significantly so.
(20) Riehl, J.-F. Thèse d'Université, 1991, Université de Paris-Sud. To be published.
(21) Hay, P. J.; Wadt, W. R. *J. Chem. Phys.* **1985**, *82*, 299.
(22) Vourwillwe, Y.; Mijoule, C.; Nizam, M.; Barthelat, J.-C.; Daudey, J.-P.; Pélissier, M.; Silvi, B. *Mol. Phys.* **1988**, *65*, 295.
(23) Stevens, W. J.; Basch, H.; Krauss, M. *J. Chem. Phys.* **1984**, *81*, 6026.
(24) Dunning, T. H. *J. Chem. Phys.* **1970**, *53*, 2823.
(25) Huzinaga, S. J. *J. Chem. Phys.* **1965**, *42*, 1293.

Table V. Bond Angles (deg) in $IrHCl_2(H_2)(P^iPr_3)_2$

Cl1–Ir–Cl2	87.0(2)	C1–P1–C7	104.5(4)
Cl1–Ir–P1	95.0(2)	C4–P1–C7	102.8(4)
Cl1–Ir–P2	96.5(2)	Ir–P2–C10	117.3(5)
Cl1–Ir–HIr1	78.0(6)	Ir–P2–C13	110.5(4)
Cl1–Ir–HIr2	120.3(7)	Ir–P2–C16	110.7(4)
Cl1–Ir–HIr3	170.2(6)	C10–P2–C13	112.5(5)
Cl2–Ir–P1	91.3(2)	C10–P2–C16	103.8(5)
Cl2–Ir–P2	91.0(2)	Cl3–P2–C16	100.7(5)
Cl2–Ir–HIr1	164.9(7)	P1–C1–C2	115.4(6)
Cl2–Ir–HIr2	152.7(7)	P1–C1–C3	114.1(5)
Cl2–Ir–HIr3	83.3(6)	C2–C1–C3	107.6(5)
P1–Ir–P2	168.5(3)	P1–C4–C5	114.9(5)
P1–Ir–HIr1	88.8(7)	P1–C4–C6	115.7(5)
P1–Ir–HIr2	85.5(7)	C5–C4–C6	110.3(5)
P1–Ir–HIr3	85.2(5)	P1–C7–C8	111.0(5)
P2–Ir–HIr1	91.9(7)	P1–C7–C9	113.6(5)
P2–Ir–HIr2	87.3(7)	C8–C7–C9	109.5(6)
P2–Ir–HIr3	83.8(5)	P2–C10–C11	111.6(8)
HIr1–Ir–HIr2	42.3(9)	P2–C10–C12	116.9(7)
HIr1–Ir–HIr3	111.8(9)	C11–C10–C12	106.1(8)
HIr2–Ir–HIr3	69.4(9)	P2–C13–C14	114.5(7)
Ir–P1–C1	115.8(4)	P2–C13–C15	117.7(7)
Ir–P1–C4	111.5(4)	C14–C13–C15	110.8(8)
Ir–P1–C7	111.2(3)	P2–C16–C17	112.1(6)
C1–P1–C4	110.0(4)	P2–C16–C18	114.4(6)
		C17–C16–C18	108.3(6)

Inelastic Neutron Scattering Study. Experiments were carried out with approximately 1 g of the *cis* isomer of $IrHCl_2(\eta^2\text{-}H_2)(P^iPr_3)_2$ on the cold neutron time-of-flight spectrometer MIBEMOL at the Orphee reactor of the Laboratoire Leon Brillouin (CE-Saclay, France). The best energy resolution that could be achieved was 0.13 cm^{-1} fwhm with an incident neutron wavelength of 12 Å. Under these conditions, however, the maximum value of the momentum transfer that can be reached is less than 1 $Å^{-1}$. At this value, the inelastic rotational form factor for the dihydrogen ligand[27] is about 20% of its maximum value, which will make the rotational tunneling transitions still harder to observe, given that their intensity is typically 0.1–0.5% of that of the elastic peak.

Results

Background. We have previously reported[7] that the reversible equilibrium in eq 3 is established in solution, with the reaction lying to the left at 290 K and to the right at 170 K. At intermediate

$$\underset{\mathbf{1}}{IrHCl_2P_2} + H_2 \rightleftharpoons \underset{\mathbf{2}}{IrHCl_2(H_2)P_2} \qquad (3)$$

$$P = P^iPr_3 \text{ or } PCy_3$$

temperatures, ^1H NMR spectra show dynamic behavior (line broadening and coalescence). Even at and above 290 K, the resonance of free H_2 is broadened perceptibly due to a small concentration of $IrHCl_2(H_2)P_2$. A remarkable feature is that the deuterated species $IrHCl_2(D_2)P_2$ does not show significant exchange between coordinated D_2 and H–Ir after 5 h. This is best explained by a *trans* structure (Scheme I), where the mutually *trans* positions of H and D_2 limit the ease of such exchange.[28]

In toluene solution under H_2, $IrHCl_2P_2$ slowly reacts further, and within several hours at 50 °C, the new product $IrH_3Cl_2P_2$ was detected and characterized. Establishing the structure of this product was difficult because of temperature-dependent ^1H NMR behavior and because these spectra were also altered by the presence or absence of H_2. We previously[7] assigned structure A to this compound, in part because it subsequently lost HCl to form $Ir(H)_2ClP_2$. We now report a more detailed study of this system, which includes a new definitive assignment of structure

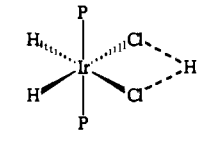

A

for this product and solid-state (diffraction) structural characterization of two species in this reaction system.

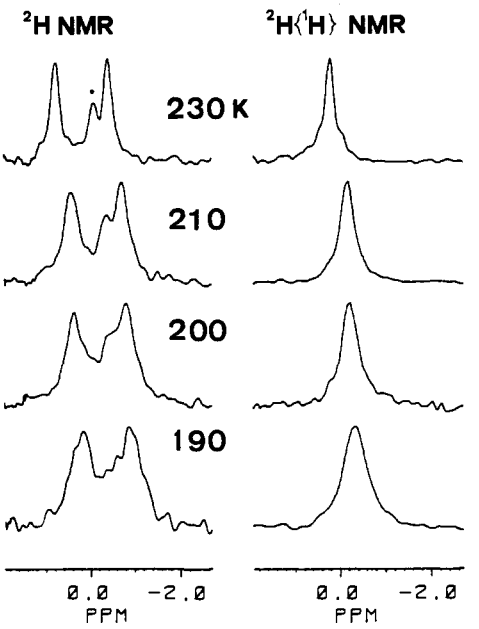

Figure 1. Variable-temperature ^2H (left) and $^2H\{^1H\}$ (right) NMR spectra of **1** dissolved in CH_2Cl_2 under an atmosphere of HD at 190 K. The signal marked by the asterisk is due to D_2 impurity. The difference $\delta(DH) - \delta(D_2)$ is about 0.25 ppm at 230 K and results from an isotope effect on the chemical shift as well as from a small isotopic perturbation of equilibrium. Proton decoupling was applied in a CW mode at the δ values of the ^2H resonances.

Scheme I

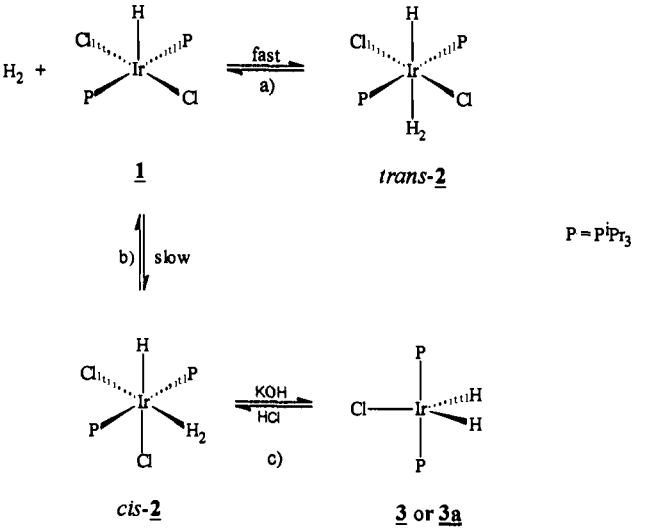

Coordination of H_2 to 1. Figure 1 shows the 190 K ^2H NMR spectrum of a CH_2Cl_2 solution of $IrHCl_2P_2$ ($P = P^iPr_3$) after reaction with HD. The deuterium chemical shift observed at –0.34 ppm essentially duplicates that reported earlier[7] for the deuterons of $IrHCl_2(D_2)P_2$. Such an assignment to $IrHCl_2(HD)P_2$ (*trans*-**2**) confirms the earlier finding that scrambling of the IrH

(26) Schmitt, M. W.; Baldridge, K. K.; Boatz, J. A.; Jensen, J. H.; Koseki, S.; Gordon, M. S.; Nguyen, K. Al; Winndus, T. L.; Elbert, S. T. GAMESS (General Atomic and Molecular Electronic Structure System). *QCPE Bull.* **1990**, *10*, 52.

(27) Eckert, J.; Heidemann, A.; Kubas, G. J., unpublished.

(28) Because of exchange and/or relaxation rate effects, it has not been possible to observe the ^1H NMR signal of coordinated H_2 in *trans*-**2**, although the corresponding ^2H NMR signal of D_2 has been detected at –0.3 ppm.

and Ir(HD) sites is slow on the NMR time scale. Consistent with the idea that the reaction in eq a (Scheme I) is a fast equilibrium, the HD ^2H NMR signal undergoes a shift to higher frequencies (free HD resonates at 4.5 ppm) when the solution is warmed. The ^2H NMR doublet for coordinated HD exhibits a large $-J_{(H-D)}$ value of 34 Hz at 190 K characteristic[29,30] of a weakly coordinated intact molecular HD ligand in *trans*-**2**. Continuous-wave ^1H decoupling collapses this doublet to a singlet. Equilibrium **a** makes the doublet splitting slightly temperature dependent; it increases to 36 Hz at 230 K.[31]

Two Isomeric Compounds of Formula $IrH_3Cl_2(P^iPr_3)_2$. In addition to equilibrium **a**, there exists a second slower ($t_{1/2} \sim 6$ h at 290 K) reaction in solution containing $IrHCl_2P_2$ and H_2. This reaction was previously reported under thermal[7] and photochemical[32b,33] conditions. Both earlier publications report elemental analysis consistent with a product of the formula $H_nIrCl_2P_2$. Reference 7 reports preliminary X-ray diffraction results indicating partial (non-hydrogen) structure **B** for this product. We now report results that permit assignment of this

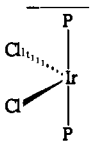

B

second reaction as equilibrium **b** (Scheme I).

It was possible to establish (Table I) that the two compounds (**1** and *cis*-**2**[34]) are in equilibrium in toluene-d_8 at and above 290 K by a study of the ^1H NMR spectra after thermostating to a reproducibly constant concentration ratio (see entries under Ar at 56 °C). Some of these ratios were reached from decreasing as well as increasing temperatures. Once equilibrated, the mole ratio of **1**-to-*cis*-**2** is quite stable at these temperatures for the duration of these experiments; the NMR spectra show no appreciable generation of other products. Only a trace of **1** is present at 290 K. In accord with the expectation that entropy will control the equilibrium concentrations, the proportion of **1** increases at higher temperatures. Also, solutions involving only autogenous H_2 (i.e., solutions equilibrated under Ar) showed a higher proportion of **1** than those under 1 atm of H_2.

Dehydrohalogenation of *cis*-$IrHCl_2(H_2)P_2$. The H_2 complex *cis*-$IrHCl_2(H_2)P_2$ can be induced to eliminate HCl. For example, *cis*-**2** rapidly reacts with CO to form *cis*,*trans*-$Ir(H)_2Cl(CO)(P^iPr_3)_2$.[7] Compound *cis*-**2** is also rapidly converted to $IrH_2Cl(P^iPr_3)_2$ (**3**) by KOH.[7] Figure 2 exhibits the 221 K ^1H NMR spectrum after brief (3 min) contact of *cis*-**2** with KOH in toluene and shows assignment of resonances. We have also observed some conversion of *cis*-**2** into **3** after addition of *cis*-**2** to toluene saturated with water. This reaction can also be reversed: dihydride **3** reacts with HCl to regenerate *cis*-**2**.[35]

The ^1H NMR spectra of a solution containing *cis*-**2** and **3** (Figure 2) show typical behavior for a two-site exchange process where an increase in $\Delta\delta$ of the two exchanging sites leads to an

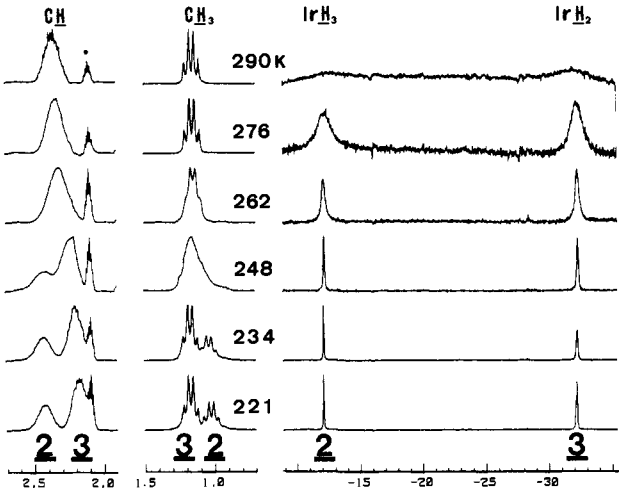

Figure 2. Variable-temperature ^1H NMR spectra of 36% *cis*-**2** with 64% **3** in toluene-d_8. The total concentration is about 0.04 mol/L. The signal marked by the asterisk is due to the solvent.

increase in the coalescence temperature.[36] Thus, averaging of resonances is observed at 248 and 262 K for CH_3 ($\Delta\delta$ = 32 Hz) and CH ($\Delta\delta$ = 46 Hz) protons, respectively. However, the influence of the site exchange on the hydride resonances is only seen as line broadening at higher temperatures due to the large difference in chemical shifts ($\Delta\delta$ = 4000 Hz). Since this solution contains equimolar H_2O from the synthesis of **3** (from *cis*-**2** and KOH), we suggest that the dynamic process involved is that shown in eq 4.[37]

$$\underset{cis\text{-}\mathbf{2}}{H_2O + IrHCl_2(H_2)P_2} \rightleftharpoons [H_3O]Cl + \underset{\mathbf{3}}{Ir(H)_2ClP_2} \quad (4)$$

Structure Determination of $Ir(H)_2Cl(P^tBu_2Ph)_2$ (3a). The stereochemistry of compound **3** was of interest to fully define the present reaction network. Our first success in large crystal growth was with the P^tBu_2Ph analog of **3**, and since its spectroscopic parameters are comparable to those of **3**, we collected neutron diffraction data. The resulting structure of $IrClH_2(P^tBu_2Ph)_2$ is shown in Figure 3. The geometry of the complex is distorted trigonal bipyramidal with the phosphine ligands occupying the apical sites. The equatorial ligands (HIr1, HIr2, Cl) and the iridium atom are nearly coplanar (angle between the HIr1–Ir–Cl and HIr2–Ir–Cl planes = 8.6°). The axial ligands are slightly displaced from their idealized positions (P1–Ir–Cl = 93.1°, P2–Ir–Cl = 94.5°). The Ir–P bond lengths are identical (Ir–P1 = 2.325 Å, Ir–P2 = 2.326 Å). The Ir–H bond lengths (Ir–HIr1 = 1.512 Å, Ir–HIr2 = 1.553 Å) are within the range of other Ir–H terminal bonds.[38] The Ir–HIr2 bond distance is longer than the Ir–HIr1 bond distance, consistent with its position more opposed to Cl. The Ir–Cl bond (2.410 Å) is shorter than those observed in six-coordinate Ir(III) complexes *trans* to one hydride ligand (around 2.5 Å)[38] and may indicate some degree of multiple bonding. The P–C bonds are staggered with respect to the equatorial ligands (Figure 4) with a ^{t}Bu group of each phosphine almost *anti* to the Ir–Cl bond (dihedral C221–P2–Ir–Cl = 162.2°, C121–P1–Ir–Cl = 163.8°) as in $RhH_2Cl(P^iPr_3)_2$.[39] The phenyl rings are almost eclipsing the P–Ir bonds (C112–C111–P1–Ir = 28.9°, C212–C211–P2–Ir = 20.9°) so that one of the *ortho* hydrogens of each ring points toward the equatorial plane (Figure

(29) (a) Kubas, G. J. *Acc. Chem. Res.* **1988**, *21*, 120. (b) Crabtree, R. H.; Hamilton, D. G. *Adv. Organomet. Chem.* **1988**, *28*, 299.

(30) (a) Earl, E. A.; Jia, G.; Maltby, P. A.; Morris, R. H. *J. Am. Chem. Soc.* **1991**, *113*, 3027. (b) Bampos, N.; Field, L. D. *Inorg. Chem.* **1990**, *29*, 587.

(31) The J_{HD} value in free HD is 43 Hz. See: Nageswara Rao, B. D.; Anders, L. R. *Phys. Rev.* **1965**, *140*, A112.

(32) (a) Mura, P.; Segre, A.; Sostero, S. *Inorg. Chem.* **1989**, *28*, 2853. (b) Bergamini, P.; Sostero, S.; Traverso, O.; Mura, P.; Segre, A. *J. Chem. Soc., Dalton Trans.* **1989**, 2367.

(33) It has been reported[32b] that photolysis of $IrHCl_2(P^iPr_3)_2{\cdot}H_2$ in CH_2Cl_2 gives three products, one of which was assigned as *cis*-**2**.

(34) Spectral data are reported in ref 7. See also Figure 2.

(35) $PtX_2(PEt_3)_2$ adds HX reversibly to give $PtHX_3(PEt_3)_2$ (X = Cl, Br, I). See: Anderson, D. W. W.; Ebsworth, E. A. V.; Rankin, D. W. H. *J. Chem. Soc., Dalton Trans.* **1973**, 854.

(36) Oki, M. *Applications of Dynamic NMR Spectroscopy to Organic Chemistry*; VCH Publishers: Deerfield Beach, 1985; Chapter 1.

(37) A referee prefers coalescence via the bimolecular intermediate $HClP_2Ir(\mu\text{-}Cl)(\mu\text{-}H)_2IrP_2(H_2)Cl$. We have independent evidence (to be published) that such bimolecular reactions do occur, but on a time scale too slow to explain the spectra in Figure 2.

(38) Robertson, G. B.; Tucker, P. A. *J. Am. Chem. Soc.* **1982**, *104*, 317.

(39) Harlow, R. L.; Thorn, D. L.; Baker, R. T.; Jones, N. L. *Inorg. Chem.* **1992**, *31*, 993.

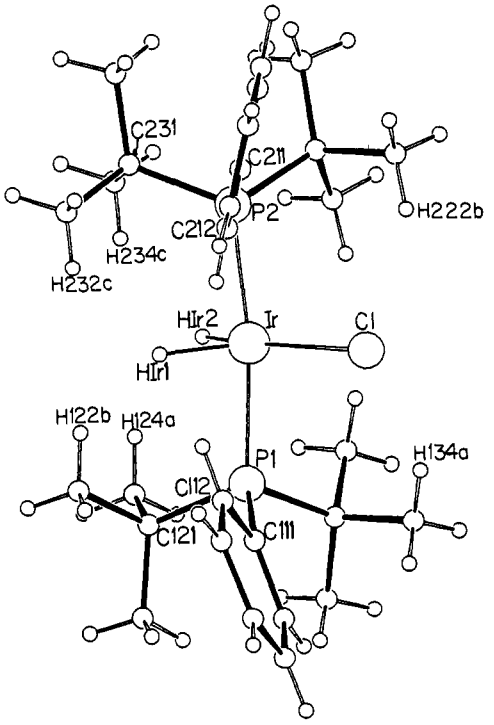

Figure 3. ORTEP drawing of $Ir(H)_2Cl(P^tBu_2Ph)_2$ (**3a**).

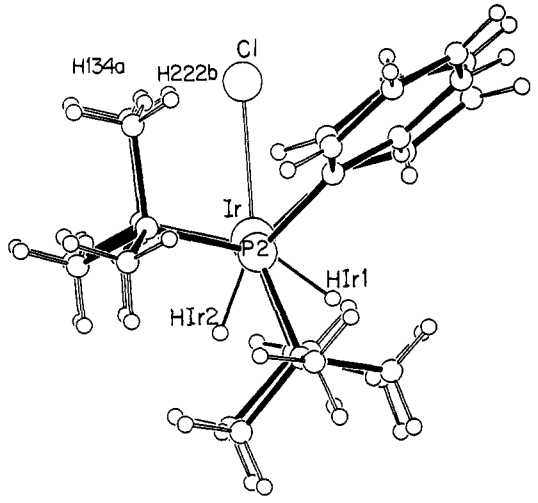

Figure 4. ORTEP drawing of $Ir(H)_2Cl(P^tBu_2Ph)_2$ viewed down the P–Ir–P axis.

3). This orientation is imposed by the bulky neighboring ^{t}Bu groups (Figure 4). These phosphines thus create a protecting screen around the equatorial plane.[40]

Within the equatorial plane (Figure 4), the H–Ir–H angle is acute (72.7°, but the H/H distance is nonbonding, at 1.82 Å) and the two obtuse H–Ir–Cl angles are unequal (HIr1–Ir–Cl = 131.1°, HIr2–Ir–Cl = 156.2°) (Figure 4). Thus, the $IrClP_2$ plane does not bisect the H–Ir–H angle. This same distortion is observed in $RhH_2Cl(P^tBu_3)_2$.[41]

The presence of an acute angle and two obtuse ones (i.e., a Y shape) has been observed in several five-coordinate d^6 complexes containing a π-donor in the equatorial plane. The acute angle in the other structures[42] is similar to that observed here. Five-coordinate d^6 trigonal-bipyramidal complexes are subject to a Jahn–Teller distortion resulting in either a square-based pyramid

(40) ^{t}Bu C–C bonds all adopt the staggered conformation of each alkyl in each phosphine.

(41) Yoshida, T.; Otsuka, S.; Matsumoto, M.; Nakatsu, K. *Inorg. Chim. Acta* **1978**, *29*, L257.

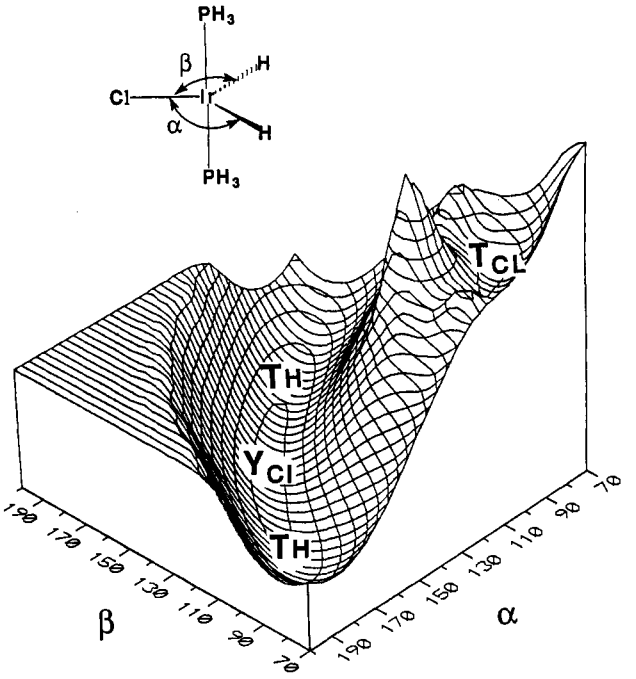

Figure 5. HF *ab initio* PES $E = f(\alpha,\beta)$ for $IrH_2Cl(PH_3)_2$. The Ir–P bonds are perpendicular to the IrH_2Cl plane.

(T shaped) or Y shape (with an acute angle between two equatorial ligands).[43,44] The Y-shaped geometry is of lower energy than the T-shaped geometry when the equatorial plane contains a single π-donor ligand X. The X ligand is then situated at the foot of the Y (Y_X) and the presence of a metal–X multiple bond is at the origin of the preference for this Y-shaped geometry. In the absence of a single π-donor ligand (or as we will see later in the presence of two π-donor ligands) a square-based pyramidal structure is calculated to be more stable.

The structure calculated at the *ab initio* level of $IrH_2Cl(PH_3)_2$ was found to have C_{2v} symmetry with excellent agreement between calculated and observed ∠H–Ir–H.[45] However, the unexpected displacement away from C_{2v} symmetry in $IrH_2Cl(P^tBu_2Ph)_2$ needs to be explained. The cause of the displacement of the Ir–Cl bond away from the C_2 axis of the H–Ir–H moiety lies in the shape of the potential energy surface $E = f(\alpha,\beta)$ (Figure 5) where α and β are the two Cl–Ir–H angles.[44] Thus, while Y_{Cl} is the absolute minimum, T_H (not a minimum) lies only 3.3 kcal/mol higher. It can be seen that Y_{Cl} lies at a bottom of a valley which remains very shallow for $\alpha + \beta$ approximately constant. This constraint corresponds to the angle H–Ir–H being nearly constant (opening by less than 15°) and is precisely the distortion observed experimentally. Thus, the position of the two hydrides can vary with respect to the Ir–Cl bond without much cost in energy *provided* that the H–Ir–H angle remains close to 73°. Weak (steric) forces are thus sufficient to cause the observed distortion. In contrast, the opening of the H–Ir–H angle forces the system to climb up the steep sides of the valley toward the high energy T_{Cl} geometry.

The relative energetic proximity of Y_{Cl} and T_H is an important property of the potential energy surface of $IrH_2Cl(PH_3)_2$. The difference in energy between Y_{Cl} and T_H comes from a combination of several factors involving the σ and π framework acting in opposite directions. The T-shaped structure is preferred over

(42) (a) Werner, H.; Hohn, A.; Dziallas, M. *Angew. Chem., Int. Ed. Engl.* **1986**, *25*, 1090. (b) Fryzuk, M. D.; MacNeil, P. A.; Boll, R. G. *J. Am. Chem. Soc.* **1986**, *108*, 6414. Fryzuk, M. D.; MacNeil, P. A.; Massey, R. L.; Boll, R. G. *J. Organomet. Chem.* **1989**, *328*, 231.

(43) Rachidi, I. E-I.; Jean, Y.; Eisenstein, O. *New J. Chem.* **1990**, *14*, 671.

(44) Daniel, C.; Kosa, M.; Han, J.; Fu, X. Y.; Morokuma, K. *J. Am. Chem. Soc.* **1988**, *110*, 3773.

(45) Riehl, J.-F.; Jean, Y.; Pélissier, M.; Eisenstein, O. *Organometallics* **1992**, *11*, 729.

the Y-shaped structure when the non-phosphine ligands are pure σ-donor since in the latter structure the $x^2 - y^2$ orbital is antibonding with the ligand *trans* to the acute angle (**4a**) while in the former case the xy is nonbonding with respect to all non-phosphine ligands (**4b**). However, the difference in energy is small (3 kcal/mol in the case of $IrH_3(PH_3)_2$). One should expect that the energy of the metal–ligand σ bonds should somewhat depend on the nature of X due to the difference in *trans* effects between H and X which in turn should play a role on the T/Y preference. The major change between the T_H and Y_{Cl} structures comes, however, from the π interaction. T_H has little π donation from Cl since the only empty available orbital (**5a**) is high in energy and poorly suited for π-type overlap. In contrast, Y_{Cl} is stabilized by the Ir–Cl π bond (**5b**). Since Cl is a poor π donor, the loss of the Ir–Cl π bond going from Y_{Cl} to T_H does not result in a great destabilization in energy.[46]

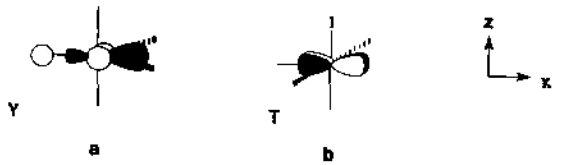

4

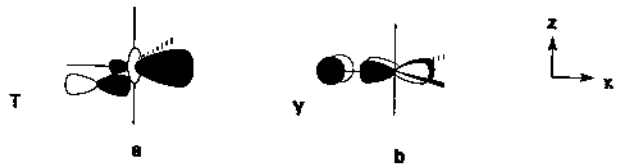

5

The shallow valley running along the constant $\alpha + \beta$ value is surrounded by steep walls which correspond to the opening of the H–Ir–H angle. Even if one of the Cl–Ir–H angles is equal to 140° (optimal value in Y_{Cl}), the opening of the H–Ir–H angle leads to a strong destabilization in energy. This is due to the fact that $x^2 - y^2$ becomes more antibonding with one of the two H's (**6**). This distortion leads to a structure closer to a TBP, a highly unfavorable geometry in the d^6 case.

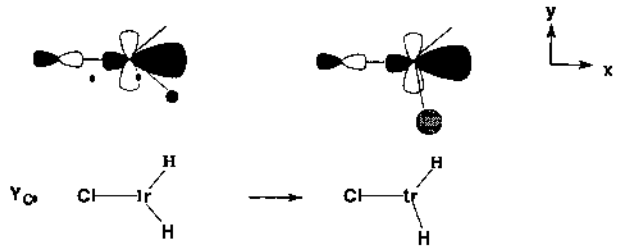

6

The shape of the valley in the PH_3 model compound *permits* distortion of the Cl–Ir–H angles but does not establish its *cause* in the experimental (P^tBu_2Ph) case. Short nonbonded contacts exist between one of the hydrides (H1r1) and one H of each ^{t}Bu group transoid to the Ir–Cl bond. In the solid-state structure, the two distances H1r1···H122b = 1.99 Å and H1r1···H232c = 2.00 Å are shorter than the sum of the van der Waals radii (2.2 Å). The other hydride is further removed from the closest H (H1r2···H234c = 2.13 Å and H1r2···H124a = 2.20 Å from methyl hydrogens) and at the limit of the van der Waals contact. If one swings only the two H's around the Ir center so that the P1, P2, Ir, Cl plane bisects the H–Ir–H angle, the shorter nonbonded distance H1r1···H122b decreases to 1.89 Å since H1r1 moves away from Cl, i.e., toward ^{t}Bu. During this motion, the other hydride moves away from the closest hydrogens so that no new short nonbonded contact appears. Therefore, the cause of the unequal Cl–Ir–H angles is the presence of asymmetric nonbonded interactions which force *one* of the two hydrides to move away from the ^{t}Bu group *anti* to Cl. Due to the electronic constraint (Figure 5) which links the motion of the two hydrides, the second hydride accompanies the first, although no steric constraint forces it to do so.

There are also some short contacts between the chlorine atom and hydrogen of the other two ^{t}Bu groups (Cl···H222b = 2.55 Å, Cl···H134a = 2.52 Å, sum of vdW = 2.7 Å). Although the angles Cl–Ir–P are both slightly larger than 90° (93.1° and 94.5°), any additional increase in the Cl–Ir–P angle is prevented by the electronic preference for the two apical ligands to remain perpendicular to the equatorial plane (the calculated optimal Cl–Ir–P angle in $IrH_2Cl(PH_3)_2$ is 90°). In addition, nonbonded interaction with the hydrides also prevents further opening of the Cl–Ir–P angle since it would diminish the already short distances between the hydride H1r1 and ^{t}Bu hydrogens H122b and H232c.

^{31}P and ^{1}H NMR Spectra of Partially Deuterated *cis*-2: Estimating $^1J_{(H-D)}$. Partially-deuterated *cis*-**2**, which is required for determination of $^1J_{H-D}$, can be prepared by the reaction of $IrHCl_2P_2$ with D_2. However, a more convenient approach is bubbling D_2 through a solution of *cis*-**2** containing a small amount of IrH_2ClP_2. This is effective because of eq 5 (which exchanges Ir–H with D_2 in fluxional **7**),[41] together with the acid catalyzed interconversion of *cis*-**2** and **3** (eq 4).

$$\underset{3}{Ir(H)_2ClP_2} + D_2 \rightleftharpoons \underset{7}{Ir(H)_2(D_2)ClP_2} \qquad (5)$$

The ^{31}P NMR spectra of two solutions containing different degrees of deuterated *cis*-**2** appear in Figure 6. These spectra permit determination of the extent of deuterium incorporation into *cis*-**2**. In spectra **A**(**BB**) and **B**(**BB**) in Figure 6 (recorded with ^{1}H broadband decoupling), ^{31}P chemical shifts of isotopomers of *cis*-**2** show an isotope effect; the increase of the number of D ligands leads to a downfield shift. The spectra are well resolved and allow estimation of the isotopomer ratio. Thus, according to our data, solutions **A** and **B** contain the following: (**A**) H_1 (41%), H_2D (42%), HD_2 (17%); (**B**) H_1 (6%), H_2D (25%), HD_2 (43%), D_1 (26%). Consequently, 25% and 63% of the H ligands of *cis*-**2** have been replaced by D ligands in solutions **A** and **B**, respectively. The experimental data are very close to a statistical ratio according to which solutions of *cis*-**2** containing 25% and 63% D should be composed: (**A**) H_1 (42%), H_2D (42%), HD_2 (14%), D_1 (2%); (**B**) H_1 (5%), H_2D (26%), HD_2 (44%), D_1 (25%).

The hydride-coupled ^{31}P NMR spectra **A**(**CW**) and **B**(**CW**) in Figure 6 show the expected overlapping quartet, triplet, doublet, and singlet resonances from the respective isotopomers of *cis*-**2** weighted due to the isotopomeric content in **A** and **B**.

With the deuterium content established, the ^{1}H NMR spectra can be informative of J_{H-D}, and thus whether or not *cis*-**2** contains an H_2 ligand. Figure 7 exhibits the hydride region of the ^{1}H NMR spectra of solutions **A** and **B** at 240 K. The ^{31}P NMR data predict that signals from the H_1, H_2D, and HD_2 isotopomers should appear in spectrum **A** in Figure 7 in a ratio close to 9:6:1, and indeed it shows the triplet (δ −12.72) of H_1 and a broad resonance at δ −12.68 which should be mainly assigned to H_2D. At the same time, spectrum **B** in Figure 7 is a superposition of resonances from the H_1, H_2D, and HD_2 isotopomers in an

(46) This is well supported by the fact that the difference in energy between Y_X and T_H increases with the π-donation ability of X (20 kcal/mol in the case of X = NH_2).

(47) (a) Medjati, M.; Tachibana, G. N.; Jensen, C. M. *Inorg. Chem.* **1990**, 29, 3. (b) Medjati, M.; Tachibana, G. N.; Jensen, C. M. *Inorg. Chem.* **1992**, *31*, 1827.

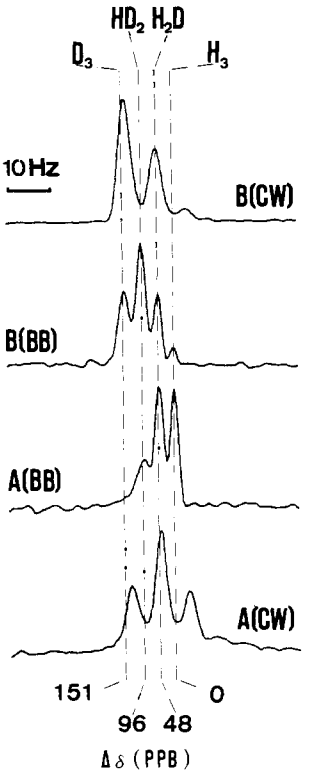

Figure 6. Hydride-coupled (CW) and decoupled (BB) ^{31}P NMR spectra of two CD_2Cl_2 solutions of partially deuterated *cis*-**2**: A, 25% D, and B, 63% D.

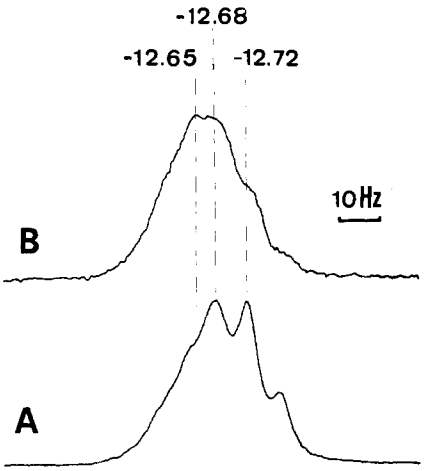

Figure 7. ^1H ligand resonances of two CD_2Cl_2 solutions of partially deuterated *cis*-**2**: A, 25% D, and B, 63% D.

approximate ratio of 2:7:6, i.e., it is mainly due to H_2D and HD_2. The increase in the amount of HD_2 isotopomer leads to further displacement of the total hydride resonance to lower field and increases intensity at −12.65 ppm. An isotope effect of this magnitude is very uncommon for hydride complexes[48,49] and can be explained by nonstatistical intramolecular distribution of D and H isotopes. In this case, if there are nonequivalent positions for the metal-bound hydrogen ligands in *cis*-**2**, at least one of them at $\delta < -12.72$ should contain more D than H isotope.[48]

Another characteristic feature of the H ligand resonances of the H_2D and HD_2 isotopomers of *cis*-**2** is the increased line width that obscures the expected H–P coupling (about 7.9 Hz). This phenomenon is especially remarkable if we take into account that

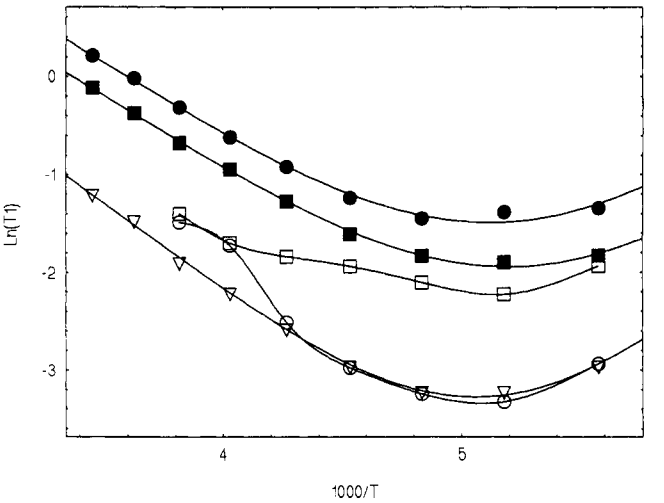

Figure 8. Temperature dependencies of spin–lattice relaxation times (T_1) for phosphine protons (●, CH_3; ■, CH) and H ligands (▽) of *cis*-**2** and T_1 data for H ligands only in a mixture of 36% *cis*-**2** (○) with 64% **3** (□). The solvent is toluene-d_8 in both cases.

(a) the typical $^2J_{(H-D)}$ constants in classical hydride complexes (about 1 Hz)[29] are less than the width of the lines of the triplet from *cis*-**2** (H_3) (3–4 Hz) and (b) a rather fast relaxation in *cis*-**2**, which is the main reason for the line width at 240 K (see below), is expected to be less efficient in *cis*-**2** (H_2D) and *cis*-**2** (HD_2).[29] The presence of an unresolved $J_{(H-D)}$ constant (in the range 1–8 Hz) can account for these features of the spectra in Figure 7. We conclude that an H_2 ligand with a *rather small* $J_{(H-D)}$ is present in *cis*-**2**.

Unfortunately, an accurate calculation of theoretical spectra for the determination of the value of $J_{(H-D)}$ requires that the relaxation time of the deuteria be known.[50] Our simulations, neglecting deuterium relaxation, have given a rough estimate of this unresolved $J_{(H-D)}$: 4 ± 1 Hz. It should be noted that in terms of a formulation of *cis*-**2** as $IrH(H_2)Cl_2(P^iPr_3)_2$, the actual $^1J_{(H-D)}$ value is three times the exchange-averaged value, i.e., about 12 $\pm$ 3 Hz.[30] A reduction of this extent from the value for free HD (43 Hz) indicates considerable Ir → (H_2) charge transfer and thus an intact H_2 ligand with considerably lengthened H–H bonds.

Temperature Dependence of Proton T_1 Relaxation Times of *cis*-2 and 3. The spin–lattice relaxation times (T_1) for the phosphine protons and metal-bound protons of *cis*-**2** and the T_1 data for the metal-bound protons in a mixture of *cis*-**2** and **3** are presented in Figure 8. For a pair of protons in an isotropically-rotating molecule, proton–proton dipole–dipole interaction determines the following rate of relaxation:[51]

$$1/T_1 = 0.3\gamma^4\hbar^2 r_{H\cdots H}^{-6}(\tau_c/(1+\omega_o^2\tau_c^2) + 4\tau_c/(1+4\omega_o^2\tau_o^2)) \quad (6)$$

$$\tau_c = \tau_o \exp(E_A/RT)$$

$1/T_1$ and $r_{H\cdots H}$ are the relaxation rate and the distance between the protons, respectively, and the other parameters are the well-known values and constants.[48,51]

In Figure 8, the lines joining the points for the mixture of *cis*-**2** and **3** have been drawn for clarity but those going through the points of *cis*-**2** are the theoretical dependencies obtained by fitting eq 6 to the different protons in the experimental data, varying r, τ_o, and E_A values.[52] As a result of the fit, E_A and τ_o values of 3.00–3.56 kcal/mol and (0.7–2.8) × 10^{-13} s have been obtained

(48) Desrosiers, P. J.; Cai, L.; Lin, Z.; Richards, R.; Halpern, J. *J. Am. Chem. Soc.* **1991**, *113*, 4173.
(49) Nanz, D.; von Philipsborn, W.; Bucher, U. E.; Venanzi, L. M. *Magn. Reson. Chem.* **1991**, *29*, S38.
(50) Leshcheva, I. F.; Torocheshnikov, V. V.; Sergeyev, N. M.; Chertkov, V. A.; Khlopkov, V. N. *J. Magn. Reson.* **1991**, *94*, 1.
(51) Abragam, A. In *The Principles of Nuclear Magnetism*; Oxford University: New York, 1971; Chapter 8.
(52) Bautista, M. T.; Earl, K. A.; Maltby, P. A.; Morris, R. H.; Schweitzer, C. T.; Sella, A. *J. Am. Chem. Soc.* **1988**, *110*, 7031.

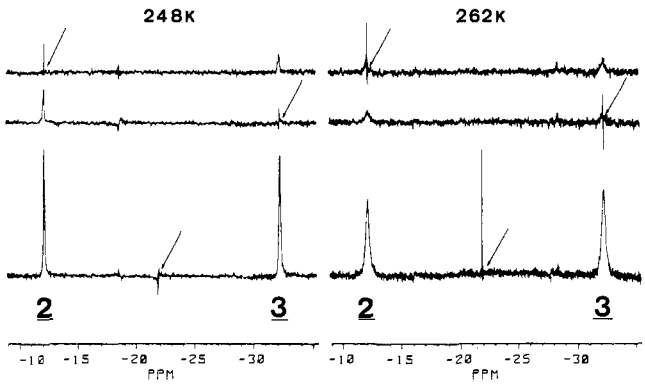

Figure 9. ^{1}H NMR spectra showing the results of saturation transfer experiments for a mixture of 36% *cis*-**2** with 64% **3** in toluene-d_8. The arrows indicate the decoupled frequencies.

and the T_{1min} times of 38 (IrH_3), 143 (CH_3), and 225 ms (CH) are determined between 193 and 198 K.

Given earlier reports[32] of paramagnetic (Ir(IV)) compounds forming from $Ir(H)_2(H_2)ClP_2$, it is important to consider the influence of paramagnetic species on these measurements. Since T_1 values are sensitive to the presence of paramagnetic impurities, it is interesting to compare T_1 data for *cis*-**2** with those for any other complex of similar geometry, i.e., rotating with τ values similar to those of *cis*-**2**.[51] To our knowledge, among a limited number of hydrides fully characterized by T_1 measurements, the dihydride $ReH_2(CO)(NO)[P(O^iPr)_3]_2$ is the complex most resembling *cis*-**2** in number of ligands and overall shape. The temperature dependence of *methyl* proton relaxation for this dihydride gives E_A = 3.2 kcal/mol, $\tau_0 = 1.7 \times 10^{-13}$ s, and T_{1min} = 120 ms (188 K) in toluene, at 200 MHz.[53] Since these values are very similar to the ones obtained for *cis*-**2**, there is no direct evidence for the occurrence of any additional relaxation contribution or of any paramagnetic Ir(IV) species.[54]

The temperature dependence of T_1 relaxation times of H ligands in the mixture of *cis*-**2** and **3** also supports the existence of equilibrium 4. At 230 K, this exchange process begins to disturb the natural course of the dependencies, and at higher temperatures the T_1 values of H ligands of *cis*-**2** and **3** are completely averaged. At 248 and 262 K, the existence of equilibrium 4 has also been confirmed by saturation transfer experiments. Figure 9 shows that when the hydride resonance of *cis*-**2** is irradiated selectively, the saturation of the resonance of **3** occurs and *vice versa*.

Figure 8 shows that, below 215 K, equilibrium 4 is slow enough to cause no influence on T_1, and a T_{1min} value of 108 ms for dihydride **3** can be considered to be due to intramolecular dipole–dipole interactions. In this case, the relaxation rate is a sum:

$$1/T_{1min} = 1/T_{1min}(H\cdots H) + 1/T^*_{1min}$$

where $1/T_{1min}(H\cdots H)$ is a contribution from dipole–dipole interaction between H ligands, and $1/T^*_{1min}$ is a contribution from dipole–dipole interactions of the H ligands with the other magnetic nuclei in **3** (mainly the phosphine protons). Thus, at 200 MHz, the distance between the H ligands in **3** is:[30,48] $r_{H\cdots H} = 2.405[T_{1min}(H\cdots H)]^{1/6}$. The T_{1min} and $r_{H\cdots H}$ values for complex **3** can be easily calculated because a value between 3 and 5 s^{-1} is a very reliable estimate of T^*_{1min}, at 200 MHz.[48,53] This approach gives $r_{H\cdots H}$ of 1.83 ± 0.06 Å, which compares to 1.82 Å from our neutron diffraction result.

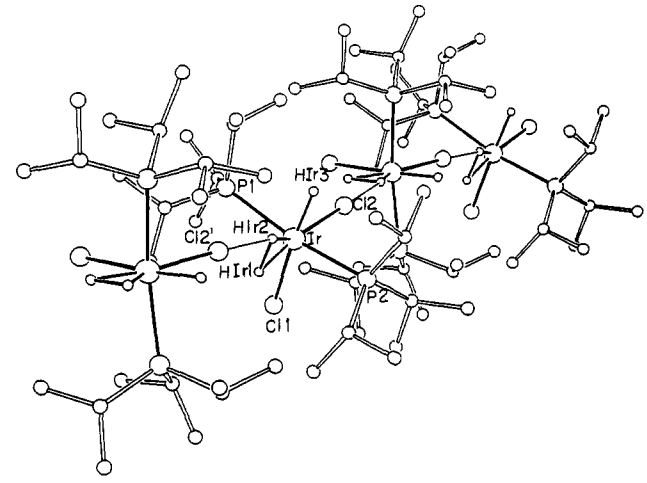

Figure 10. Crystal packing of *cis*-$Ir(H)Cl_2(H_2)(P^iPr_3)_2$ showing the infinite chains along the *a* axis.

Taken together, the data presented above make it unlikely that the T_1 times for the hydride resonance of *cis*-**2** are shortened due to paramagnetic relaxation. The T_{1min} value of 38 ms at 200 MHz is appreciably shorter than those of classical hydrides (in the absence of significant metal–H dipole–dipole interactions)[48] and gives evidence of H–H bonding between the IrH_3 ligands in *cis*-**2**. Using the common approach,[30a,48] the T_{1min} value of 38 ms was used to calculate the H–H distance in the dihydrogen ligand of $IrH(H_2)Cl_2(P^iPr_3)_2$: 1.07 ± 0.01 and 1.35 ± 0.02 Å are the lower and upper limits of r_{H-H} assuming rapid and slow intramolecular spinning of the H_2 ligand, respectively. The rapid rotation value is distinctly closer to the neutron diffraction result (1.11 Å, see below).[55]

The absence of paramagnetic relaxation in the $Ir(H)_2Cl(P^iPr_3)_2$ and $IrHCl_2(H_2)(P^iPr_3)_2$ solutions studied here is further supported by the T_{1min} value measured for $Ir(H)_2Cl(P^tBu_2Ph)_2$. T_{1min} is proportional to field strength when dipole–dipole relaxation is the dominant relaxation mechanism.[48] The T_{1min} of the hydrides of $Ir(H)_2Cl(P^tBu_2Ph)_2$ was determined as 239(4) ms at 243 K and 500 MHz. Assuming that dipole–dipole relaxation is the dominant relaxation mechanism, the T_{1min} at 200 MHz would be (2/5) × 239(4) ms = 96(2) ms. This value is similar to the T_{1min} value of 108 ms determined for the hydrides of $Ir(H)_2Cl(P^iPr_3)_2$.[56] Since there is no evidence for paramagnetic species in $Ir(H)_2Cl(P^tBu_2Ph)_2$, the good agreement between T_{1min} of this compound and that of $Ir(H)_2Cl(P^iPr_3)_2$ further supports the absence of significant paramagnetic impurities in the latter.

Structure Determination of *cis*-$IrHCl_2(H_2)(P^iPr_3)_2$. The ORTEP drawing of $Ir(H)Cl_2(H_2)(P^iPr_3)_2$ (*cis*-**2**) is shown in Figure 10. The structural study confirms that there has been an

(53) Gusev, D. G., unpublished results.

(54) Solution proton and ^{31}P NMR observations on this same system have been interpreted by Mura *et al.*[32a] in terms of equilibrium a (Scheme I) *together with* traces of a paramagnetic species $Ir^{IV}(H)_2Cl_2P_2$. Although EPR signals were detected in solution, the NMR spectra showed no significantly altered chemical shifts, and the EPR spectra were not subjected to spin counting. Two X-ray crystal structures were also reported (P^iPr_3 and PCy_3 analogs); these were refined (including hydrogen) as an Ir^{IV} dihydride; each molecule possesses a crystallographic center of symmetry. However, in view of the fact that the P^iPr_3 example adopts the same space group shown twice recently to involve disorder of mutually *trans* ligands, we feel that both $Ir(H)_2Cl_2P_2$ species would also give satisfactory refinements as $IrHCl_2(H_2)P_2$ or $IrHCl_2P_2$, or a co-crystallized mixture of the two (i.e., a solid solution, with infinitely variable composition *and color*). See: Harlow, R. L.; Thorn, D. L.; Baker, T.; Jones, N. L. *Inorg. Chem.* **1992**, *31*, 993. Dunbar, K. R.; Haefner, S. C. *Inorg. Chem.* **1992**, *31*, 3676. We are informed by C. A. Jensen that this is indeed the case (to be published). While a definitive proof will require duplication of all of the measurements made by the Mura group, we feel that the equilibria among diamagnetic species proposed in our present report satisfactorily accounts for our chemical shift, dynamic NMR, and T_1 observations.

(55) In the absence of fast dihydrogen spinning in *cis*-$IrH(H_2)Cl_2P_2$, the HIr–HIr2 and HIr2–HIr3 distances (1.11 and 1.78 Å, respectively) predict a T_{1min} value for the exchange-averaged IrH3 resonance of 13.7 ms. This is much shorter than the experimental T_{1min} of 38 ms. Thus, assuming dihydrogen spinning accounts for the lengthening of T_{1min}, the expected rotational barrier must be less than the barrier for the overall molecular reorientation, i.e., less than 3 kcal/mol.

(56) The fact that the T_{1min} for the hydride of $Ir(H)_2Cl(P^tBu_2Ph)_2$ at 200 MHz is slightly smaller than the T_{1min} determined for $Ir(H)_2Cl(P^iPr_3)_2$ may be explained by a larger relaxation contribution ($1/T^*_{1min}$) from closer phosphine ligand hydrogens of the larger (cone angle 170° vs 160°) di-*tert*-butylphenylphosphine.

isomerization which places the chlorides mutually *cis*, and also brings the hydride *cis* to H_2. Interligand angles are close to 90°, and the Ir–Cl distance *trans* to hydride (2.496(6) Å) is longer than that *trans* to H_2 (2.445(6) Å) consistent with the larger *trans* effect of the hydride. The Ir–hydride distance (1.584(13) Å) is not significantly different from the distance of Ir to the H_2 hydrogens (1.537(19) and 1.550(17) Å). This is an unprecedented situation and indicates strong binding of the molecular hydrogen. Consistent with this conclusion, the H–H distance within the molecular H_2 ligand, 1.11(3) Å, is the longest yet determined[57] accurately (i.e., by neutron diffraction); this indicates a large degree of backbonding into σ^*_{H-H}. The H_2 ligand lies in the $IrHCl_2$ plane. This conformation is favored since it aligns the σ^*(H–H) orbital with the highest d orbital (destabilized by one lone pair of each chlorine). This conformation also benefits from a stabilizing *cis* interaction involving weak interaction between the occupied σ_{Ir-H} orbital and σ^*_{H-H}.[58] The two *cis* ligands (Cl1 and H) are slightly bent away from H_2 (170.2(6)°). This is also an unusual situation, and such bending is diagnostic of strong binding of H_2 to Ir. Bending of the *cis* ligands has the effect of increasing back-donation into σ^*_{H-H}.

The final significant structural element is the occurrence of intermolecular hydrogen bonding between HIr2 and Cl2′. This interaction (2.64(2) Å, compared to the sum of van der Waals radii of 2.7 Å) links the molecules (weakly) into an infinite chain polymer along the *a* axis in the solid state. Such hydrogen bonding is a vivid demonstration of the Brønsted acidity of coordinated H_2. Intermolecular nonbonding interactions between the bulky phosphines within the infinite chain are avoided by having the P–Ir–P axis of adjacent molecules in the staggered conformation. The *ab initio* calculation (see below) indeed gives a positive charge on the two H's of the coordinated dihydrogen ligand. Note also that the chlorine has enhanced nucleophilic character because its two p lone pairs are interacting with two of the occupied t_{2g} orbitals of Ir (Cl lone pair/Ir(d_π)). *Intramolecular* hydrogen bonding is also possible between HIr1 and Cl1 (2.65 Å). For comparison, the HIr3–Cl2 distance is 2.76 Å. This intramolecular hydrogen bond may provide an alternative mechanism for conversion of $IrHCl_2(H_2)P_2$ to $Ir(H)_2ClP_2$ + HCl.

Dynamics of H_2 Rotation in *cis*-$IrHCl_2(H_2)P_2$. In some of our previous work[58-62] we were successful in obtaining an experimental value for the height of the barrier to rotation of the dihydrogen ligand. This is accomplished by inelastic neutron scattering measurements of rotational transitions of the dihydrogen ligand and subsequent analysis with a simple model for this rotation,[60] namely in-plane rotation in a double-minimum potential. The origin of this barrier lies primarily in the variation of the backbonding interaction $d_\pi(M) \rightarrow \sigma^*(H_2)$ as the dihydrogen ligand rotates in a plane perpendicular to the Cl–Ir–H_2 axis. The barrier height may therefore be considered to be a measure of the degree of backbonding[61,63] in the ground state *relative* to that in the least stable rotated form.

The rotational energy levels for a hindered rotor subject to low-to-medium barriers consist of a series of split librational levels.[60,64] Of particular importance is the rotational tunnel splitting of the librational ground state, as it depends exponentially on the barrier height and is therefore the most sensitive measure thereof. An observation of this transition alone is sufficient for obtaining the 2-fold potential barrier height for this simple model.

A search for the rotational tunneling transitions of *cis*-$IrHCl_2(H_2)(P^iPr_3)_2$ yielded no discrete excitations between the elastic peak and about 30 cm^{-1}, which is *well above the largest known rotational tunnel splitting*[65] *for dihydrogen complexes.* We must therefore conclude that the rotational tunneling transition is too small to be observable with the spectrometer used, and we will therefore simply be able to place a lower limit on the barrier height.

On the basis of the knowledge of the intensities of the tunneling transitions from our previous work on other dihydrogen complexes and the instrumental resolution (measured with a sample of polyethylene), we can estimate that the smallest observable rotational tunnel splitting would have been approximately 0.08 cm^{-1}. If we then use the d(H–H) value of 1.11 Å obtained in our neutron diffraction study, we can calculate the value of the rotational constant B as 26.5 cm^{-1}. With this value for B and the upper limit on the observable rotational tunnel splitting, the lower limit for a 2-fold barrier to rotation of dihydrogen in $IrHCl_2(H_2)(P^iPr_3)_2$ would be 2.0 kcal/mol. Since it is likely that the value for d(H–H) obtained in our neutron diffraction study needs to be corrected for thermal motion (as was done in ref 65, and discussed in ref 62), the actual value of B would be somewhat lower than the above. This will have the effect of reducing the lower limit we can place on the barrier height since the scale of the rotational energy levels is given by B. We do, however, expect that the thermal motion correction to d(H–H) in the present case would be considerably less than that for $Mo(CO)(H_2)(dppe)_2$ (ref 65) because of the stronger backbonding interaction in *cis*-**2**.

The lower limit on the barrier of 2.0 kcal/mol is in any case in agreement with our much larger calculated value of 6.5 kcal/mol. In addition, the experimentally-determined barrier is likely to contain a contribution from the hydrogen bonding described above which increases the barrier to rotation.

Isomeric Structures *trans*-2 and *cis*-2 ($IrH(H_2)Cl_2P_2$). Coexistence of a pair of H_2 complexes isomeric by virtue of the stereochemistry at the metal is rare.[66] We consider here the bonding factors which govern this condition for the Ir(III) system under study.

(a) Conditions for the Existence of Two Isomers. The coordination of H_2 to a transition metal fragment has been examined at several levels of theory.[67] Most of the interest has focussed on the orientation of H_2 with respect to the metallic fragment and on the activation of H_2 leading to a dihydride complex. The possibility of structurally isomeric forms of the metal/ligand fragment to which H_2 binds has been neglected.[67c] This is, however, an important aspect of the chemistry of the present system since it may permit us to understand competitive reaction pathways (i.e., Scheme I). We will show that in the case of a hexacoordinated H_2 complex, metal/ligand stereochemistry can influence the orbital energies of the fragment to which H_2 binds and therefore the total energy of the isomeric H_2 complexes.

(57) We consider that the 1.36 Å H/H separation reported in $ReH_7[P(p\text{-tolyl})_3]_2$ no longer represents an H_2 molecule. See: Brammer, L.; Howard, J. A. K.; Johnson, O.; Koetzle, T. F.; Spencer, J. L.; Stringer, A. M. *J. Chem. Soc., Chem. Commun.* **1991**, 241.

(58) Van der Sluys, L. S.; Eckert, J.; Eisenstein, O.; Hall, J. H.; Huffman, J. C.; Jackson, S. A.; Koetzle, T. F.; Kubas, G. J.; Vergamini, P. J.; Caulton, K. G. *J. Am. Chem. Soc.* **1990**, *112*, 4831.

(59) Eckert, J. *Spectrochim. Acta* **1992**, *48A*, 363.

(60) Eckert, J.; Blank, H.; Bautista, M. T.; Morris, R. H. *Inorg. Chem.* **1990**, *29*, 747.

(61) Eckert, J.; Kubas, G. J.; Hall, J. H.; Hay, P. J.; Boyle, C. M. *J. Am. Chem. Soc.* **1990**, *112*, 2324.

(62) Eckert, J.; Albinati, A.; White, R. P.; Bianchini, C.; Peruzzini, M. *Inorg. Chem.* **1992**, *31*, 4241.

(63) Eckert, J.; Kubas, G. J. *J. Phys. Chem.*, submitted for publication.

(64) See, for example: Press, W. *Single Particle Rotations in Solids*; Springer Verlag: Berlin, 1981; Springer Tracts in Modern Physics, Vol. 92.

(65) Kubas, G. J.; Burns, C. J.; Eckert, J.; Johnson, S. W.; Larson, A. C.; Vergamini, P. J.; Unkefer, C. J.; Khalsa, G. R. K.; Jackson, S. A.; Eisenstein, O. *J. Am. Chem. Soc.* **1993**, *115*, 569. Eckert, J.; Albinati, A.; White, R. P.; Bianchini, C.; Peruzzini, M. *Inorg. Chem.* **1992**, *31*, 4241.

(66) For other examples, see: Jessop, P. G.; Morris, R. H. *Coord. Chem. Rev.* **1992**, *121*, 260.

(67) See the following, and references cited therein: (a) Jean, Y.; Eisenstein, O.; Volatron, F.; Maouche, B.; Sefta, F. *J. Am. Chem. Soc.* **1986**, *108*, 6587. Riehl, J. F.; Pélissier, M.; Eisenstein, O. *Inorg. Chem.* **1992**, *31*, 3344. (b) Hay, P. J. *J. Am. Chem. Soc.* **1987**, *109*, 705. Eckert, J.; Kubas, G. J.; Hall, J. H.; Hay, P. J.; Boyle, C. M. *J. Am. Chem. Soc.* **1990**, *112*, 2324. (c) Burdett, J. K.; Mohammed, R. P. *Organometallics* **1987**, *6*, 1684. Burdett, J. K.; Phillips, J. R.; Mohammed, R. P. *Inorg. Chem.* **1987**, *26*, 3054. (d) Pacchioni, G. *J. Am. Chem. Soc.* **1990**, *112*, 80. Maseras, F.; Duran, M.; Lledos, A.; Bertran, J. *J. Am. Chem. Soc.* **1991**, *113*, 2879; **1992**, *114*, 2922. (e) Lin, Z.; Hall, M. B. *J. Am. Chem. Soc.* **1992**, *114*, 6102 and 2928.

Two interactions are responsible for the binding of H_2 to the transition metal fragment. The σ_{H2} orbital interacts with an empty metal σ orbital to make the metal–H_2 σ bond. Back-donation occurs from a filled nonbonding orbital of the ML_5 fragment into the empty σ^*_{H-H}. The strengths of these two interactions determine the metal–H_2 bond energy and the nature of the bonding (H_2 vs two hydrides). A metal σ orbital of low energy gives a strong metal–H_2 σ bond. Strong backbonding from an electron-rich metal causes the cleavage of the H–H bond and leads to a dihydride structure. Let us now discuss the conditions for the existence of two isomers.

Suppose that the square-pyramidal $MXX'L_3$ fragment is bonded to H_2 in two different ways so that it is either X (T_X) (**9**) or X′ ($T_{X'}$) (**10**) which is *trans* to H_2. This describes the difference

9 10

between *cis*- and *trans*-**2**. The total energy (E) of these two isomeric H_2 adducts can be written as follows:

For the $T_X(H_2)$ isomer

$$E(T_X(H_2)) = E(T_X) + E(H_2) + E_{int} \quad (7)$$

where $E(T_X)$ is the energy of the five-coordinate T_X metal fragment with X *trans* to the empty site of the square pyramid, $E(H_2)$ is the energy of H_2 with the H–H bond distance in the complex, and E_{int} is the interaction energy.

For the $T_{X'}(H_2)$ isomer

$$E(T_{X'}(H_2)) = E(T_{X'}) + E'(H_2) + E'_{int} \quad (8)$$

with similar definitions for the new energy terms and where $T_{X'}$ is now the five-coordinate metal fragment with X′ *trans* to the empty site of the square pyramid.

If the two H_2 adducts are both complexes of molecular H_2 with comparable H–H distances, then $E(H_2) \approx E'(H_2)$. Furthermore, since the $M(H_2)$ bond energy is small,[68] the two values for the interaction of H_2 with the metal cannot be very different and it is reasonable to assume $E_{int} \approx E'_{int}$. In such a situation, the total energy of the two H_2 isomeric adducts can be dictated by the relative energy of the two square-pyramidal fragments. A large energy difference between the two square-pyramidal fragments leads to a large energy difference between the two H_2 adducts; the isomer where H_2 is linked to the more stable T fragment should predominate. If, on the other hand, the energy of the two T fragments is similar, two isomeric H_2 adducts can be expected to coexist. In this case, the more stable isomeric H_2 adduct does not necessarily correspond to the more stable square-pyramidal fragment since small differences between the values of E_{int}/E'_{int} and $E(H_2)/E'(H_2)$ can influence the relative total energy.

It has been shown that the more stable square pyramid is the one which has the best σ-donor ligand *trans* to the empty site. Large differences in σ-donating ability (i.e., in *trans* effect) should lead to metal fragments with a large energy difference and the expectation of one highly preferred isomeric H_2 adduct. This argument, however, only focuses on the ability of the ligand *trans* to the empty site to determine the energy of the fragment and totally neglects the role of the other (spectator) ligands in modifying the energy of the fragment; this assumption may be inappropriate. This will be illustrated by the comparison between $Ir(H)_2Cl(H_2)P_2$ where only one isomer has been detected[47] and $IrHCl_2(H_2)P_2$, under study here, where two isomers (H_2 *trans* to H or Cl) are observed. We will show how the change in the "spectator" ligand (H vs Cl) drastically modifies the relative energies of the two square-pyramidal fragments (T_H and T_{Cl}) and therefore the relative energies of the H_2 adducts.

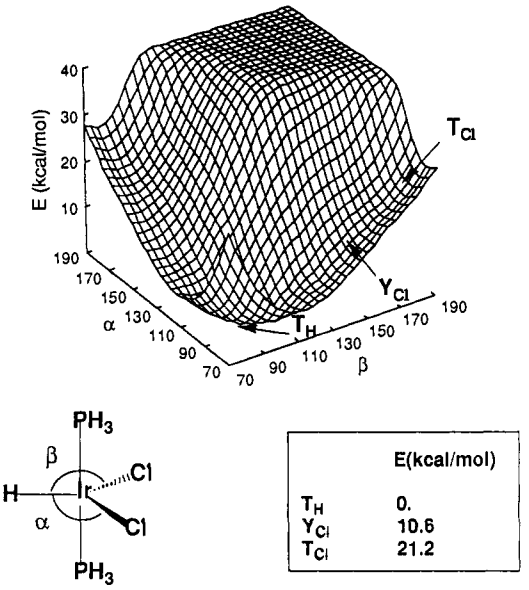

Figure 11. Plot of HF *ab initio* PES $E = f(\alpha,\beta)$ for $IrHCl_2(PH_3)_2$. The Ir–P bonds are perpendicular to the IrH_2Cl plane. T_H: $\alpha = 90°$, $\beta = 90°$. T_{Cl}: $\alpha = 90°$, $\beta = 180°$ and $\alpha = 180°$, $\beta = 90°$.

(b) The case of $Ir(H)_2Cl(H_2)(PH_3)_2$. For this monochloride species, two six-coordinate isomers can be constructed $T_H(H_2)$ and $T_{Cl}(H_2)$. Ab *initio* calculations show that T_H is more stable than T_{Cl} by 35.3 kcal/mol in agreement with the larger *trans* effect of the hydride.[45] This large difference in energy suggests that $T_H(H_2)$ should be considerably more stable than $T_{Cl}(H_2)$, which is indeed the case. $T_{Cl}(H_2)$ was calculated to be 28.1 kcal/mol less stable than $T_H(H_2)$.[67e] Although the H centers have not been found in the X-ray diffraction study of $Ir(H)_2Cl(H_2)P_2$ (P = P^iPr_3), the assumption that H_2 is *trans* to a hydride ligand has never been questioned.[47]

This discussion also applies to $FeH(dppe)_2(H_2)^+$. From a neutron diffraction study, it is known that H and H_2 are *trans* and from study in solution it has been shown that the exchange between the three H centers is slow.[69] In this case, our EHT calculations of $FeH(PH_3)_4^+$ show that T_H is considerably more stable than T_{PH3} leading to a more stable $T_H(H_2)$ adduct.[70] This result is in agreement with the fact that H has a stronger *trans* effect than phosphine.

(c) The Isomeric Structures of $IrHCl_2(H_2)(PR_3)_2$. The plot of *ab initio* potential energy surface (PES) $E = f(\alpha,\beta)$ (Figure 11) for the five-coordinate $IrHCl_2(PH_3)_2$ shows a global minimum around $\alpha = 90°$ and $\beta = 90°$, which corresponds to the T_H square-pyramidal structure. Selected structural parameters of the fully optimized structure given in Figure 12 show that the system is a square pyramid. This result is in agreement with the structure of $RhHCl_2(P^iPr_3)_2$.[38] No other minima are found on this surface. However, two valleys describing the opening of the H–Ir–Cl angle (increasing α or β) rise in energy only gently. T_{Cl} which is a high point in this valley is calculated to be 21.2 kcal/mol above T_H. Therefore, the six-coordinate $T_H(H_2)$ might be expected to be more stable than $T_{Cl}(H_2)$. Our *ab initio* calculations of the optimization of the H_2 adducts show that this is *not* the case and that $T_{Cl}(H_2)$ is 10.3 kcal/mol more stable than $T_H(H_2)$.[71]

(68) Gonzalez, A. A.; Zhang, K.; Nolan, S. P.; Lopez de la Vega, R.; Mukerjee, S. L.; Hoff, C. D.; Kubas, G. J. *Organometallics* **1988**, *7*, 2429.

(69) Ricci, J. S.; Koetzle, T. F.; Bautista, M. T.; Hofstede, T. M.; Morris, R. H.; Sawyer, J. F. *J. Am. Chem. Soc.* **1989**, *111*, 8823. Bautista, M. B.; Earl, K. A.; Morris, R. H. *Inorg. Chem.* **1988**, *27*, 1124. Bautista, M. B.; Earl, K. A.; Morris, R. H.; Sella, A. *J. Am. Chem. Soc.* **1987**, *109*, 3780.

(70) In all our systems, the results from EHT and *ab initio* calculations show similar qualitative trends.

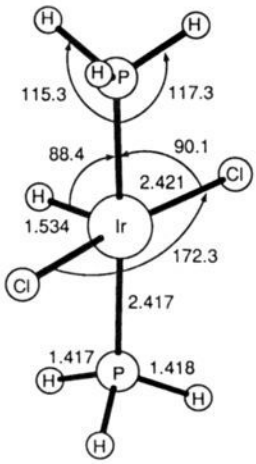

Figure 12. Selected structural parameters of the fully (HF) optimized geometry of $IrHCl_2(PH_3)_2$.

We will now discuss (i) why the substitution of the "spectator" ligand chloride in place of hydride reduces the energy difference between the two square-pyramidal isomers and (ii) why the energy of the H_2 adducts does not follow the energy of the square-pyramidal fragments.

The relative energy of square-pyramidal d^6 fragments is determined mainly by the σ interactions between the metal and the ligands. The hydride has a large *trans* effect and disfavors the bonding of any other ligand with a large *trans* effect *trans* to itself since two strong σ-donor ligands are then competing for the same metal orbital. In contrast, a ligand with a weak *trans* effect can be put *trans* to the hydride without causing excessive destabilization. Thus, $Ir(H)_2ClP_2$, which has two *trans* hydride ligands as T_{Cl}, is considerably higher in energy than T_H in which the two hydrides are *cis*. In contrast, the energy difference is significantly reduced (although T_H remains the more stable) in the case of $IrHCl_2P_2$ since in T_{Cl} the hydride ligand is *trans* to Cl and not H.

The interaction energy between H_2 and the metal is determined by the strength of the σ Ir–H_2 bond and of the Ir–H_2 backbonding described above. It is difficult to separate the role of these two factors. An examination of the molecular orbitals of T_H and T_{Cl} suggests the σ Ir–H_2 bond plays an important role. The LUMO of a square-pyramidal fragment (**11**) is lower in energy with a chloride than with a hydride *trans* to the empty site, again as a consequence of the reduced *trans* effect of Cl. The five-coordinate T_{Cl} metal fragment is thus a much better Lewis acid than the T_H isomer and the $Ir(H_2)$ bond is stronger in $T_{Cl}(H_2)$. The calculated

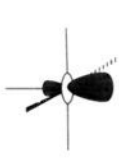

11

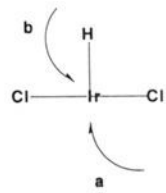

12

Ir–H_2 bond dissociation energy is[71b] 13.4 kcal/mol in $T_H(H_2)$ and 23.7 kcal/mol in $T_{Cl}(H_2)$. However, this factor can reverse the ordering given by the energy of the square-pyramidal fragments only if the two five-coordinated fragments are close in energy. This is the case for the dichloro derivative. Interestingly, the first isomer observed in our experimental studies (i.e., kinetic product) is $T_H(H_2)$, resulting from T_H being attacked by H_2 *trans* to the hydride (attack a, in **12**). Weak bonding between the metal and H_2 in this isomer favors reversibility, permitting the slower attack of H_2 *cis* to the hydride in **1** and leading finally to the more stable (thermodynamic) product (attack b, in **12**).

Discussion

Scheme I summarizes transformations observed experimentally. No direct equilibrium arrows linking *cis*- with *trans*-**2** have been drawn since we feel that, given the generally high barriers to intramolecular rearrangement of d^6 octahedra,[72] a unimolecular rearrangement mechanism cannot be competitive with the known rapid dissociation of coordinated H_2 (i.e., exchange of free and coordinated H_2 is rapid on the ^1H NMR time scale at 25 °C). Moreover, we know (NMR studies on the time scale of hours) that the production of *cis*-**2** is slow. This is quite consistent with the overwhelmingly-preferred attack trajectory of H_2 on $IrHCl_2P_2$ being *trans* to hydride in **12**, so that the kinetic product is the *less* stable H_2 adduct. In order to form the thermodynamically-preferred adduct, another attack trajectory (of higher E_a) must exist. Given that **13** is not a minimum (Figure 11), it is not possible that *cis*-**2** forms from preformed **13** (in thermal

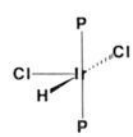

13

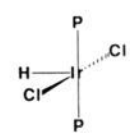

14

equilibrium with **14**). Instead, we propose that H_2 approaches **12** in the H–Ir–Cl plane and *cis* to hydride (attack b) and that the H–Ir–Cl angle increases in response to that approach. This is a more highly activated process, so it produces *cis*-**2** more slowly than does the alternative attack trajectory (*trans* to hydride) to generate *trans*-**2**. This is thus an interesting (and rare) case where a dissociative mechanism (involving full bond rupture) is better than an intramolecular rearrangement (i.e., angle bending). We suggest that bond rupture is possible because one or more π-donor ligands remain coordinated and stabilize the five-coordinate species by Cl → Ir π-bonding. This is precisely the effect invoked in the SN_1CB mechanism (eq 9).[73]

$$B + Co(H_2O)_6^{3+} \rightleftharpoons$$

$$BH^+ + Co(H_2O)_5(OH)^{2+} \rightleftharpoons H_2O + \text{(OH}_2\text{)}_4\text{Co(OH)(OH}_2\text{)}^{2+} \quad (9)$$

The presence of hydrogen bonding in solid *cis*-**2** has implications for the mechanism of eq 4. We suggest that the electron-rich character of the chlorides in *cis*-**2** (caused by d_π/Cl_π filled/filled repulsions) would cause H_2O to hydrogen bond to chloride (especially probable in benzene solvent), and thus initiate heterolytic splitting of the IrCl bond, with generation of molecular HCl. This leaves OH^- geminal with the emerging $IrH_3ClP_2^+$ ion, with the acidic character of coordinated H_2 facilitating proton

(71) (a) A partial geometry optimization of the H_2 complexes with frozen T metal fragments was performed. $T_{Cl}(H_2)$ with H–H perpendicular to P–Ir–P shows H–H = 1.4 Å and Ir–(H2) = 1.4 Å; $T_{Cl}(H_2)$ with H–H parallel to P–Ir–P shows H–H = 1.1 Å and Ir–(H2) = 1.5 Å. $T_H(H_2)$ optimized with H–H parallel to P–Ir–P and H–H = 0.81 Å and Ir–(H2) = 1.77 Å. The difference in energy between these two conformations is 2.3 kcal/mol. (b) This has been calculated as $E[T_H(H_2)] - E(H_2) - E[T_H]$ and $E[T_{Cl}(H_2)] - E(H_2) - E[T_H]$ where $E(H_2)$ is evaluated at 0.74 Å bond length. $E[T_H]$ is used for evaluating *both* bond energies since it is the only stable structure (i.e., $E[T_{Cl}]$ is not a minimum). **Added in Proof**: Coupled pair functional calculations yield a shorter H–H distance for $T_{Cl}(H_2)$ than 1.4 Å.

(72) Note that, in *cis*-**2**, forming $P_2Cl_2Ir(H)_3$, or even a trihydrogen compound $P_2Cl_2Ir(H_3)$, is not productive of isomerization to *trans*-**2** since neither of these intermediates delivers hydrogen to the other side of the surface defined by Ir, 2P, and 2Cl.

(73) Tobe, M. L. *Acc. Chem. Res.* **1970**, *3*, 377.

transfer to OH^-. The idea that protons can facilitate relief of the filled/filled repulsion in a six-coordinate $L_5Ir^{III}Cl$ species is consistent with the observation that $IrCl_3(PMe_3)_3$ in water solvent is immediately converted to Cl^- and $IrCl_2(H_2O)(PMe_3)_3^+$.[74]

Conclusions

This work shows that the five-coordinate substructures have quantitatively distinct bonding potential toward H_2. While **14** binds H_2 with only a small equilibrium constant, **13** has a significantly larger binding constant. The structure of the H_2 adduct of **13** shows (experimentally) an unusually long H–H bond, which is confirmed by *ab initio* calculations. In contrast, *ab initio* calculations show a shorter H–H bond in the H_2 adduct of **14** and a smaller Ir–H_2 bond dissociation energy. These differences originate from two factors: The strong *trans* effect of H diminishes the strength of the Ir–(H_2) σ bond in the H_2 adduct of **14**. H_2 remains far from the metal and backbonding is consequently less efficient due to a smaller overlap. Furthermore, from the calculations, the H_2 ligand prefers to eclipse the Ir–P bonds due to the destabilizing interaction of H_2 with the Cl lone pairs. The occupied d orbital in the P–Ir–P plane is not destabilized by a Cl p orbital and is therefore not a powerful back-donating orbital. The situation is very different in the H_2 adduct of **13**. The *trans* Cl has a weak *trans* effect which permits the establishment of a much stronger and shorter Ir–H_2 σ bond. Back-bonding can thus be much stronger. In addition, the H_2 ligand is preferentially in the H–$IrCl_2$ plane where the occupied d orbital is destabilized by two p Cl lone pairs.

(74) Merola, J. *Inorg. Chem.*, submitted for publication.

These results show that the *reducing power* of fragment **13** toward H_2 *greatly exceeds* that of **14**. The idea that fragment stereochemistry can influence reducing power is an important principle for the future.

Acknowledgment. V.G. thanks Professor H. Alper for support and freedom to pursue this project and Drs. A. Yanovsky and Y. Struchkov for a crystallographic study. The neutron diffraction studies and structure refinements were carried out at Brookhaven National Laboratory under contract DE-AC02-76CH00016 with the U.S. Department of Energy and supported by its Office of Basic Energy Sciences. The technical assistance of J. Guthy and C. Koehler in these studies is gratefully acknowledged. J.E. thanks the Laboratoire Leon Brillouin for the use of their facilities and Gerrit Coddens for invaluable assistance with the inelastic neutron scattering experiments. The Laboratoire de Chimie Théorique is associated with the CNRS (URA 506) and is a member of ICMO and IPCMO. This work was supported by the U.S. National Science Foundation and the French CNRS under Grants CHE-9103915 and INT-88-14838 and by material support from Johnson Matthey/Aesar. We thank the Indiana University Institute for Advanced Study for support of the visit of O.E. M.P.S. thanks the University of Thessaloniki and the CNRS for financing his stay at Orsay.

Supplementary Material Available: Tables of positional and thermal parameters for $Ir(H)_2Cl(P^tBu_2Me)_2$ and $Ir(H)_2(H_2)Cl(P^iPr_3)_2$ (6 pages); listing of structure factors (38 pages). Ordering information is given on any current masthead page.